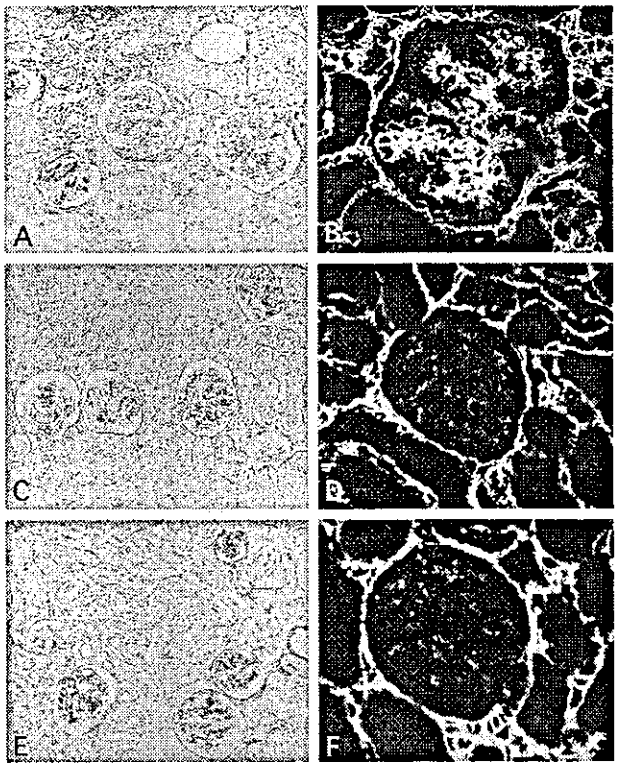

Fig. 2. Light micrographs (*A, C, E*) and immunofluorescence micrographs of anti-type I collagen (*B, D, F*) on the 56th day after mAb 1-22-3. Mesangial cell proliferation and severe matrix expansion are still detected on the 56th day after mAb 1-22-3 injection in uninephrectomized rats (A), whereas LM findings of sham operated rats were almost normalized (C). Intense staining of collagen type I was detected in the mesangial area in uninephrectomized rats injected with mAb 1-22-3 (B). The staining of collagen type I in sham operated rats was weak and focal (D). (E) and (F) show the control findings of uninephrectomized rats without injection of mAb 1-22-3 (A, C, E ×200, B, D, F ×400).

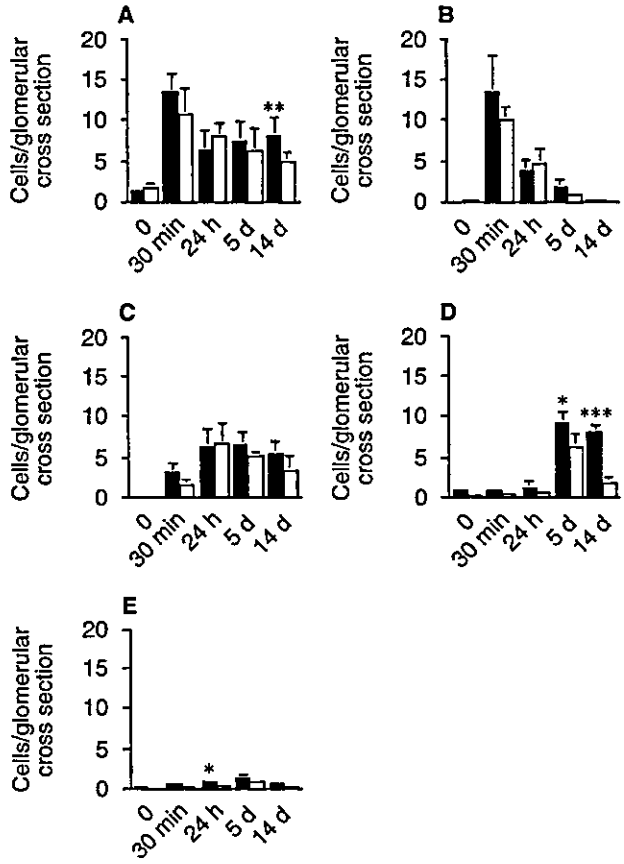

Fig. 3. Time course of the number of infiltrating inflammatory cells in glomeruli after injection of mAb 1-22-3 in the uninephrectomized group and the sham operated group. Symbols are: (■) uninephrectomized prolonged model; (□) sham-operated reversible model; $*P < 0.05$, $**P < 0.01$, $***P < 0.005$ vs. corresponding time point of sham operated model. $OX\text{-}1^+$ cells in glomeruli increased in both groups, peaked at 30 minutes and decreased gradually. (*A*) A larger number of $OX\text{-}1^+$ cells were detected on the 14th day in the uninephrectomized group than that of the sham operated group. (*B*) $RP\text{-}3^+$ cells infiltration into glomeruli peaked within 30 minutes. No significant difference of the infiltration of $RP\text{-}3^+$ cells was detected in both groups. (*C*) In the uninephrectomized group, $ED1^+$ cells infiltrated into glomeruli earlier than in the sham operated group. (*D*) Increased number of $ED3^+$ cells in glomeruli was detected on the 5th day and the 14th day in both groups. The number of $ED3^+$ cells in the uninephrectomized group was larger than that of the sham-operated group. (*E*) Few of $OX\text{-}19^+$ cells were detected in both groups.

in the uninephrectomized rats without an injection of mAb 1-22-3 during the experimental period. No difference of mesangial alteration on day 5 was observed between both groups. In the sham operated group, although mesangial morphological alterations were still detected on the 14th day, mesangial alterations were gradually decreased by the 56th day. Severe mesangial alterations were still detected on the 56th day in the uninephrectomized group. The mesangial matrix score and the IF intensity scores of α-SMA, and collagen type I on the 56th day were shown in Figure 1B. Mesangial matrix expansion in the uninephrectomized group was 3.85 times higher than that of the sham operated group. The IF intensity score of α-SMA and the collagen type I of the uninephrectomized group was 2.01, and 1.93 times higher than those of the sham group. No abnormal morphological alterations were observed in the uninephrectomized rats without injection of mAb 1-22-3. The representative findings of the light microscopy and collagen type I IF staining on the 56th day after injection are shown in Figure 2. These results support the previous report that the mesangial alteration induced by mAb 1-22-3 injection into uninephrectomized rats are prolonged.

Infiltration of inflammatory cells in glomeruli

The kinetics of the recruitment of $OX\text{-}1^+$, $RP\text{-}3^+$, $ED1^+$, $ED3^+$, and $OX\text{-}19^+$ cells were shown in Figure 3. $OX\text{-}1^+$ cells in glomeruli increased in both groups, peaked at 30 minutes after mAb 1-22-3 injection and

decreased gradually. A larger number of OX-1$^+$ cells were detected on the 14th day in the uninephrectomized group than in the sham operated group (Fig. 3A). RP-3$^+$ cells accumulated rapidly, peaked at 30 minutes after the injection of mAb 1-22-3, and had returned to normal levels by day 5. No significant difference of the infiltration of RP-3$^+$ cells was observed in both groups (Fig. 3B). In the uninephrectomized group, ED1$^+$ cells infiltrated into glomeruli earlier than in the sham operated group. However, no difference of the peak number of ED1$^+$ cells was observed in both groups (Fig. 3C). Few of ED3$^+$ cells were detected in normal glomeruli and at the early stage of the 1-22-3 induced glomerulonephritis, but the number of ED3$^+$ cells increased at the later stage (days 5 and 14) in both groups. The number of ED3$^+$ cells recruited in glomeruli in the uninephrectomized group was already significantly higher on day 5 than that of the sham operated rats ($P < 0.05$). The number of ED3$^+$ cells on the 14th day was 4.5 times higher in the uninephrectomized group than in the sham operated group (Fig. 3D). Few of OX-19$^+$ cells were detected in both groups (Fig. 3E).

mRNA expression for chemokines in glomeruli

mRNA expression of MCP-1 in the uninephrectomized group was already increased at 30 minutes (2.70 times to the normal expression) and decreased to 1.33 times at 24 hours, whereas MCP-1 mRNA expression in the sham operated group at 30 minutes is 1.99 times to the normal expression and peaked at 24 hours (2.62 times). Increased mRNA expression of the lymphotactin was detected on the fifth day in both groups. There was no significant difference of lymphotactin expression on day 5 between the uninephrectomized group (2.26 times to normal expression) and the sham operated group (2.32 times). Increased mRNA expression of the TARC was detected on the 14th day in both groups, and there was no significant difference between the uninephrectomized group (1.85 times to normal expression) and the sham operated group (1.45 times). No increased expression of RANTES was detected in both groups at any time points examined. In the uninephrectomized group, mRNA expression of the fractalkine dramatically increased on the 14th day (6.5 times to normal expression). The fractalkine expression of the uninephrectomized group was significantly higher than that in the sham operated group (2.5 times to sham operated group). The kinetics of the expression of fractalkine and a representative RT-PCR finding on the 14th day is shown in Figure 4.

Immunostaining of fractalkine

In the uninephrectomized group, clearly positive staining of fractalkine in glomeruli was already detected at 24 hours, and its intensity peaked on the 14th day (Fig. 5A). No positive staining of fractalkine was detected on

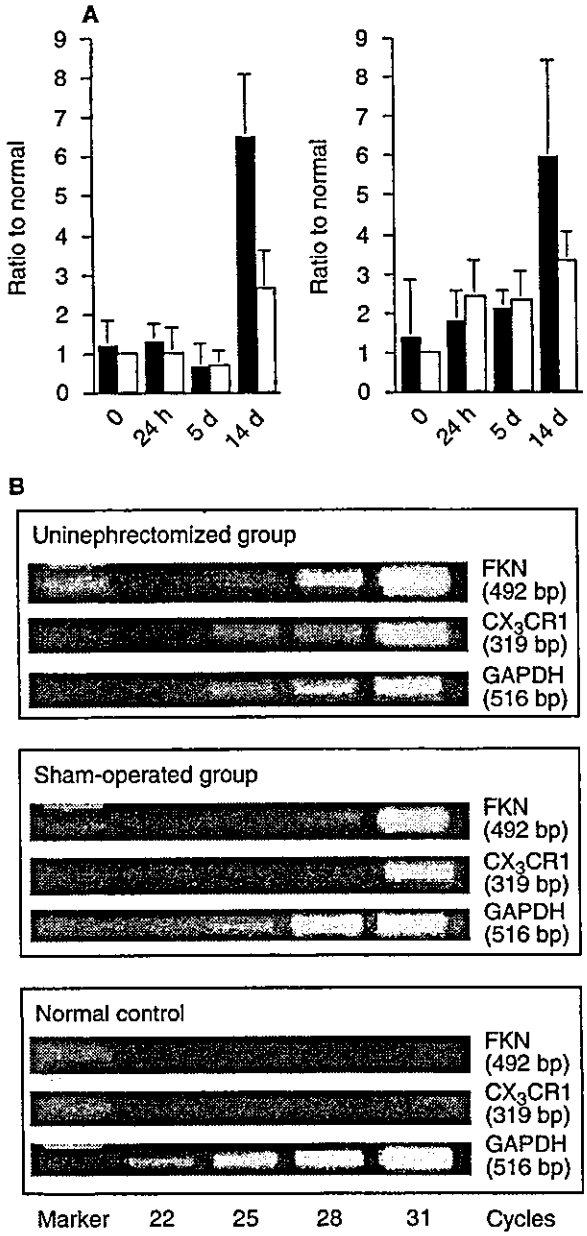

Fig. 4. Kinetics of fractalkine (FKN) and CX_3CR1 mRNA expression on the 14th day after mAb 1-22-3 injection. (*A*) mRNA expression was semiquantitated by RT-PCR using cDNA corresponding to 750 ng RNA. Symbols are: (■) nephrectomized; (□) sham-operated. The optimal cycle numbers were determined in a preliminary trial to be in the linear phase of amplification. Ratios of the densitometric signals of FKN (left panel) or CX_3CR1 (right panel) and the internal control (GAPDH) were analyzed. The data are shown as the ratio relative to normal rat findings and are expressed as mean ± SD of three independent experiments. FKN mRNA expression of uninephrectomized rats on day 14 was 2.52 times higher than that in the normal rat findings. (*B*) Representative agarose gel electrophoretic patterns of PCR products of FKN, CX_3CR1, and GAPDH on day 14 in 3 cycle intervals.

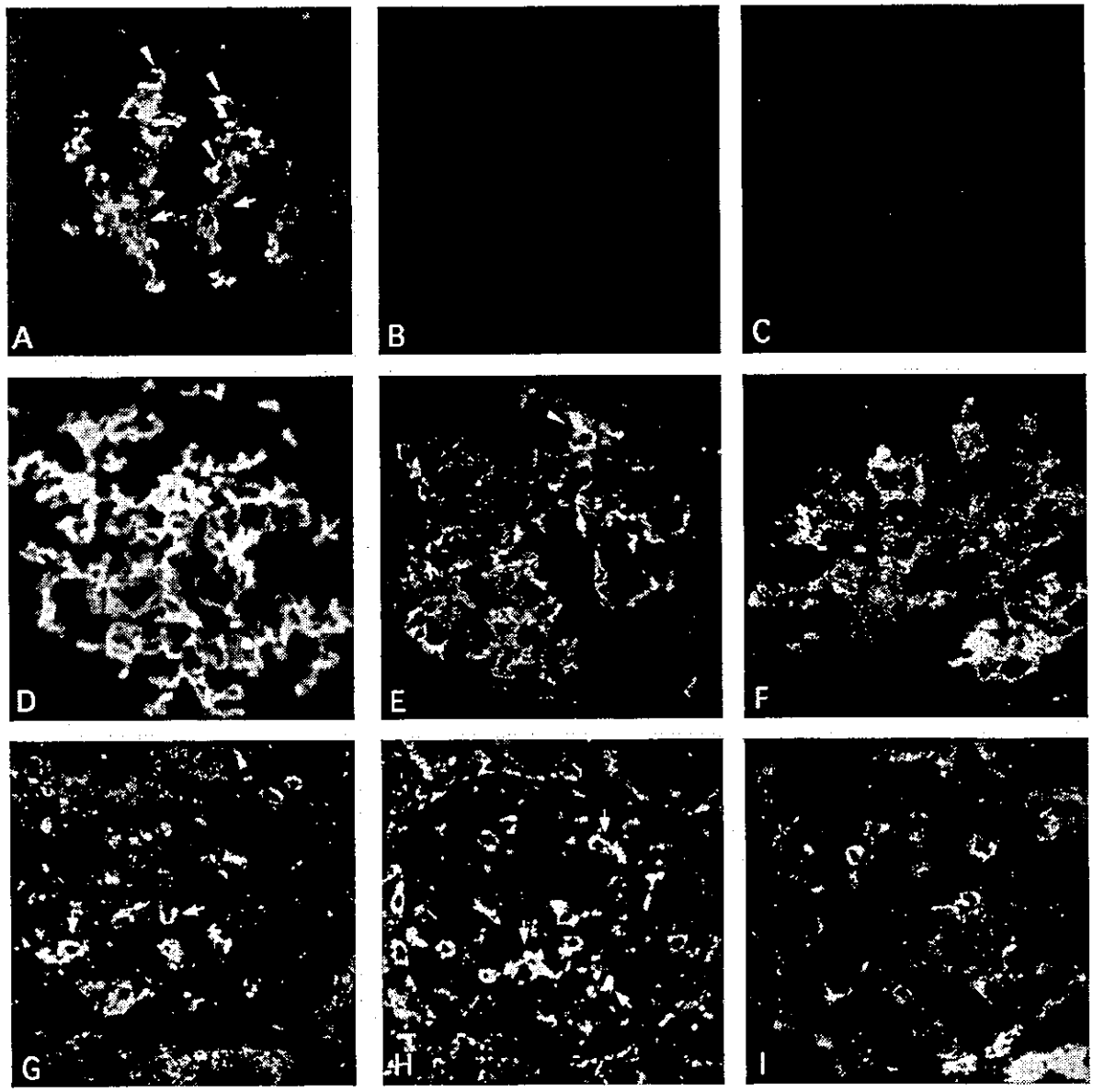

Fig. 5. Immunofluorescence findings of fractalkine (FKN) and CX_3CR1 in glomeruli after mAb 1-22-3 injection in the uninephrectomized rat. (*A*) Immunofluorescence micrograph of FKN on the 14th day after mAb 1-22-3 injection into a uninephrectomized rat. Intense staining of FKN is detected at the site facing the capillary lumen (arrowheads), and the staining is also detected at the mesangial area (arrows). (*B*) No staining is detected with anti-FKN antibody (Ab) pre-incubated with fusion protein of the extracellular site of FKN in the same rat material as used in panel A. (*C*) FKN staining is not detected in normal rat glomeruli. (*D*) Dual labeling staining with anti-FKN Ab (green) and anti-RECA1 Ab (red) on the 5th day. A part of RECA1 positive cells (endothelial cells) is positive for FKN (yellow). (*E*) Dual labeling staining with anti-FKN Ab (green) and anti-RECA1 Ab (red) on the 14th day. Positive staining of FKN is detected in endothelial cell (yellow, arrow head) and in the mesangial area (green). (*F*) Dual labeling staining with anti-FKN Ab (green) and mAb 1-22-3 (red) on the 14th day. Monoclonal antibody (mAb) 1-22-3 was used as a marker for mesangial cell. Positive staining of FKN is detected in the mesangial area (yellow). (*G*) Dual labeling staining with anti-CX_3CR1 (green) and with ED1 (red) on the 5th day. A part of the $ED1^+$ cells are also stained with anti-CX_3CR1 (yellow, arrows). (*H*) Dual labeling staining with anti-CX_3CR1 (green) and with ED3 (red) on the 5th day. Major parts of $ED3^+$ cells are also stained with anti-CX_3CR1 (yellow, arrows). (*I*) Dual labeling staining with anti-CX_3CR1 (green) and with OX-19 (red) on the 5th day. No double positive cells were detected.

the 56th day in the uninephrectomized group. Fractalkine staining in the sham operated group was weak and focal at the any of the time points examined. Fractalkine expression was not detected in the normal kidneys (Fig. 5C). On the fifth day, a part of the endothelial cells was positive for fractalkine (Fig. 5D), and fractalkine expression also was detected in the mesangial area on the 14th day (Fig. 5 E, F). No positive staining was detected with

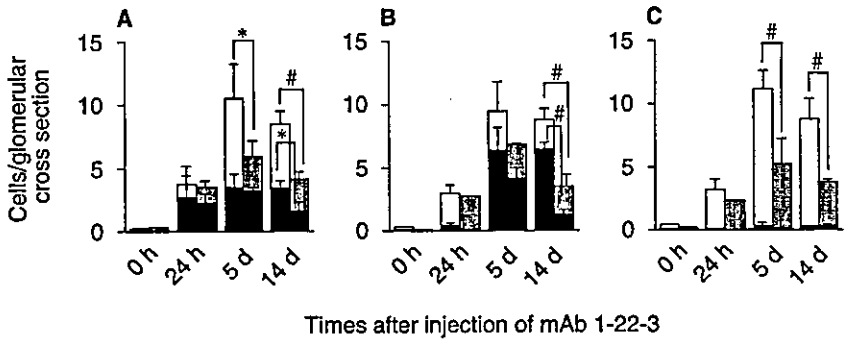

Fig. 6. Time course of number of CX_3CR1 positive cells and double positive cells co-stained with (*A*) ED1, (*B*) ED3, or (*C*) OX-19. Symbols are the numbers of: CX_3CR1-positive cells in the (□) uninephrectomized group and (▨) sham operated group; (■) double positive cells with CX_3CR1 and each macrophage and T cell marker. $*P < 0.05$, $\#P < 0.005$. Infiltration of CX_3CR1^+ cells in glomeruli peaked on the 5th day after injection of mAb 1-22-3. The number of CX_3CR1^+ cells was larger in the uninephrectomized group than in the sham operated group. The majority of the CX_3CR1^+ cells were positive for macrophage marker. Almost all CX_3CR1^+ cells were negative for T cell marker.

anti-fractalkine antibody that was pre-absorbed with fusion protein of chemotactic site of fractalkine (Fig. 5B), although positive staining was detected with anti-fractalkine antibody that was preincubated with fusion protein of pGEX-6P-1 without insert. The rate of fractalkine positive glomeruli was significantly higher in the uninephrectomized group than in the sham operated group (60 ± 17 vs. $18 \pm 13\%$, $P < 0.01$).

mRNA expression of CX_3CR1 and identification of CX_3CR1 expressing cells

Increased mRNA expression of CX_3CR1 was already detected at 24 hours in the uninephrectomized group. The CX_3CR1 mRNA expression in the uninephrectomized group on the 14th day was significantly higher than that in the sham operated group. The kinetics of the expression of CX_3CR1 and a representative RT-PCR finding on the 14th day is shown in Figure 4. The expression of CX_3CR1 mRNA was decreased to almost normal level on 56th day. The dual labeling of the immunofluorescence findings of the anti-CX_3CR1 with ED1, ED3, or OX-19 is shown in Figure 5 (G-I), and the kinetics of the double positive cells of CX_3CR1 and ED1, ED3, or OX-19 is in Figure 6. The number of CX_3CR1^+ cells in glomeruli peaked on the fifth day and were significantly increased in the uninephrectomized group (1.42 times more to the number of sham operated groups on day 5). The majority of the CX_3CR1^+ cell was positive for macrophage marker: 66.7% of the CX_3CR1^+ cells were $ED3^+$ cells on the fifth day and 73.9% on the 14th day in the prolonged model. On the other hand, 69.5% of $ED3^+$ macrophages in glomeruli on the fifth day in the prolonged model were positive for CX_3CR1, and 80.7% on the 14th day.

Chemotaxis analysis of inflammatory leukocytes from nephritic glomeruli

The mean numbers of leukocytes on the undersurface of the filter attracted by fractalkine or PBS/BSA were

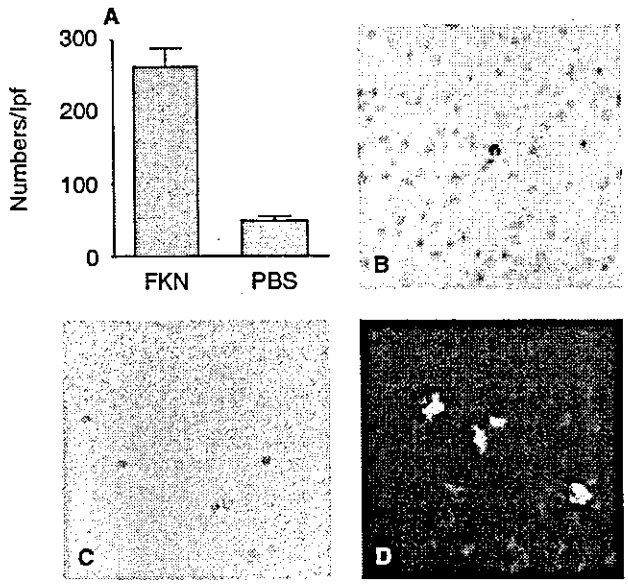

Fig. 7. Chemotaxis of glomerular leukocytes to fractalkine (FKN). Chemotaxis of inflammatory leukocytes isolated from glomeruli of rats injected with mAb 1-22-3 to FKN was assayed. The mean numbers of migratory cells per low power field (×200) on the undersurface of the filter were shown (*A*). The representative Giemsa staining specimens of the inflammatory leukocytes migrated to undersurface of the filter of the chamber with FKN (*B*), and of the chamber with PBS/BSA only (*C*). (*D*) Immunofluorescence finding of the filter with ED3 shows that $ED3^+$ cells were attracted by FKN (B, C ×200; D ×400).

shown in Figure 7A. The representative finding of Giemsa staining specimens of the cells attracted by fractalkine and the finding of negative control with PBS/BSA were shown in Figure 7 B and C, respectively. Figure 7D shows that a part of leukocytes attracted by fractalkine was $ED3^+$ cells.

Effect of candesartan on the expression of fractalkine and the recruitment of CX_3CR1^+ cells

We confirmed that the candesartan treatment ameliorated the matrix score at six weeks after disease induction

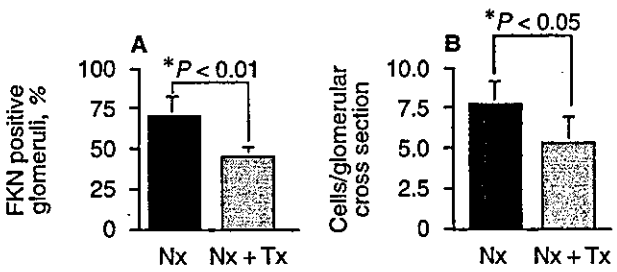

Fig. 8. Comparison of fractalkine (FKN) expression and the recruitment of CX_3CR1^+ cells in the glomeruli between candesartan-treated (Nx + Tx) and non-treated rats (Nx). The rate of FKN positive glomeruli (*A*) and the number of CX_3CR1^+ cells in glomeruli (*B*) on the 14th day after mAb 1-22-3 injection into uninephrectomized rats was determined. FKN expression and the number of CX_3CR1^+ cells in glomeruli were significantly decreased by treatment with candesartan.

(0.38 ± 0.096 vs. 1.40 ± 0.16 candesartan treatment vs. PBS treatment, $P < 0.01$). However, the candesartan treatment did not ameliorate the matrix score on day 14 (1.22 ± 0.133 vs. 1.23 ± 0.068, candesartan treatment vs. PBS treatment). There were no significant differences of C_{Cr} or serum creatinine on the 14th day between candesartan and PBS treated groups (candesartan treatment vs. PBS treatment, 4.20 ± 0.59 vs. 4.38 ± 0.35 mL/min/kg body wt; serum creatinine: 0.46 ± 0.03 vs. 0.50 ± 0.04 mg/dL; serum creatinine of normal rat findings: 0.29 ± 0.05 mg/dL). Candesartan treatment did not decrease SBP on day 11 (112.64 ± 49.1 vs. 128.94 ± 24.21 mm Hg candesartan treatment vs. PBS treatment; SBP of normal rat, 129.22 ± 12.2 mm Hg). By contrast, decreased immunostaining of fractalkine was observed in the candesartan treated group on the 14th day (Fig. 8A). The number of CX_3CR1^+ cells in the glomeruli of the candesartan treated group on the 14th day was significantly less than in the PBS treated group (Fig. 8B). Decreased mRNA expressions of fractalkine and CX_3CR1 were observed in the candesartan treated group on the 14th day (Fig. 9). Real-time RT-PCR analysis also showed that decreased expression of glomerular mRNA for fractalkine in rats treated with candesartan. Although candesartan treatment decreased mRNA expression of MDS, the decrease of MDC was not so remarkable if compared with the decrease of fractalkine (Fig. 9). Candesartan treatment increased mRNA expression of MCP-1 (Fig. 9).

mRNA expression of fractalkine and CX_3CR1 in mAb1-22-3 two consecutive injections model

In the two consecutive injections model, mRNA expression of fractalkine and CX_3CR1 in the glomeruli after the second injection was higher than those after the first injection. The RT-PCR data on the 14th day after the first and second injections are shown in Figure 10.

DISCUSSION

We previously reported that a single injection of anti-Thy 1 mAb 1-22-3 [32, 33] into the uninephrectomized rats was capable of inducing the persistent proteinuria and the prolonged mesangial alterations (prolonged model) [18, 30], although the mesangial alterations induced by a single injection of mAb 1-22-3 to normal rats without uninephrectomy were reversible (reversible model) [32]. While the hemodynamic change caused by a uninephrectomy is considered to affect the outcome of the disease, the precise mechanism of the prolonged model has not been clarified yet. To compare the initiation events just after mAb 1-22-3 injection and the consequent inflammatory responses in the glomeruli between the sham operated reversible model and the uninephrectomized prolonged model is a successful way to identify the essential factor in bringing about the prolonged alterations.

First, the initiation events just after the mAb 1-22-3 injection were compared in these models. The amount of the kidney binding mAb 1-22-3 was higher in the nephrectomized group than in the sham operated group (11.3 vs. 8.55 μg/kidney; Table 1). However, our previous quantitative study with various injection doses of mAb 1-22-3 showed that there was no significant difference in the infiltrating cells and the severity of mesangial alterations between 0.5 mg injected rats (kidney binding, 7.2 μg/kidney) and 10 mg injected rats (kidney binding, 32.7 μg/ kidney) [27]. We experienced that the prolonged mesangial alterations could be induced by a half dose of mAb 1-22-3 injection into uninephrectomized rats (data not shown). We did not detect the significant differences of the complement deposition and the severity of the mesangiolysis between the nephrectomized and the sham operated models (Table 2). These observations indicate the difference of the kidney binding antibody between the sham operated and the uninephrectomized groups had little effect on the different outcomes of the disease.

Next, we compared the expression of chemokine and the recruitment of inflammatory cells in glomeruli after mAb 1-22-3 injection in the sham operated reversible model and the uninephrectomized prolonged model. Fractalkine expression of the uninephrectomized group was significantly higher than that in the sham operated group, although no difference in the expressions for MCP-1, TARC, lymphotactin, or RANTES was detected. The mRNA expression of the fractalkine on the 14th day of the uninephrectomized prolonged model was 2.5 times higher than that of the sham-operated reversible model (Fig. 4). In addition, clear positive immunostaining of fractalkine in glomeruli was detected in the uninephrectomized prolonged model at 24 hours, whereas fractalkine staining in the sham-operated reversible model was weak and focal at any time points examined.

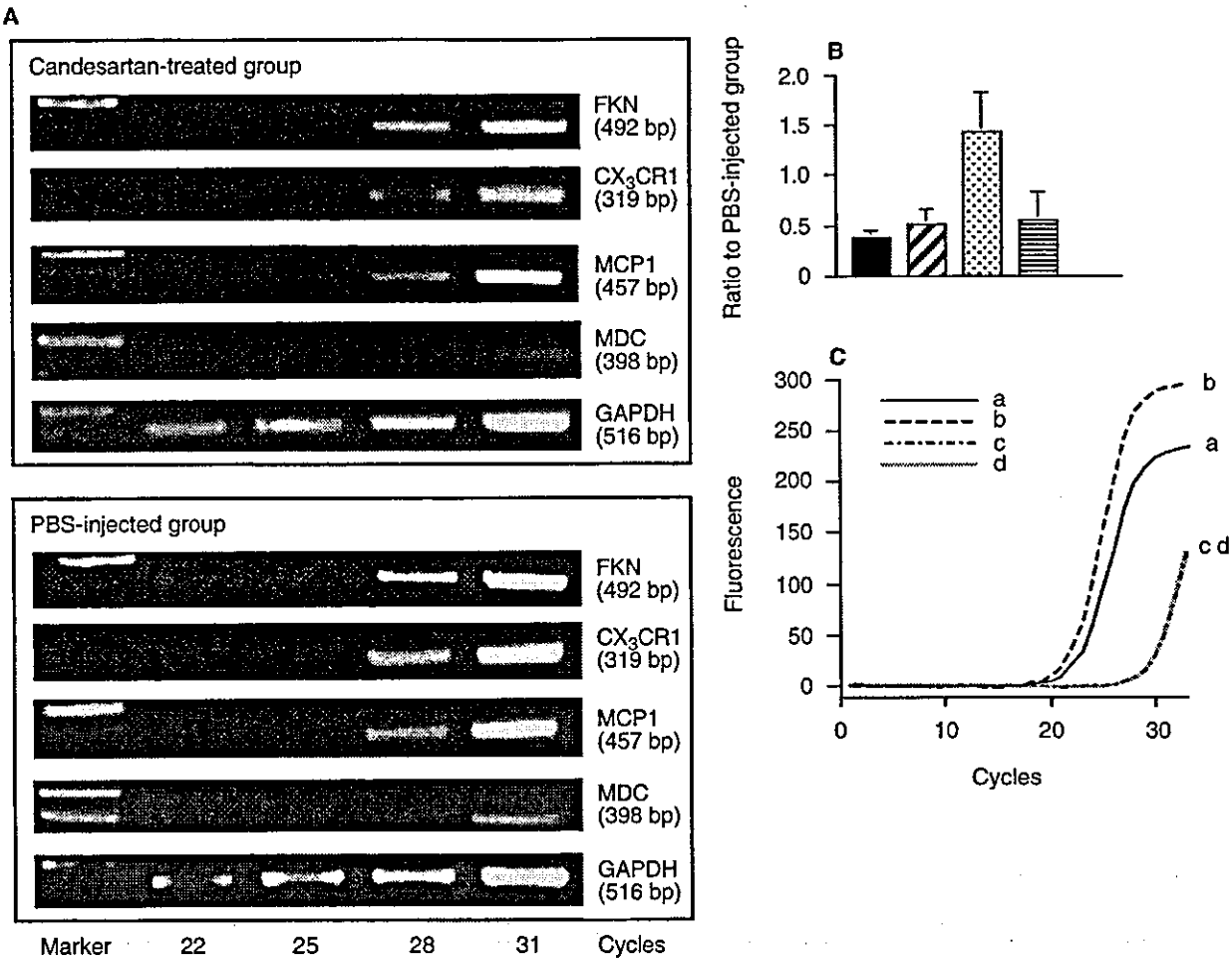

Fig. 9. Chemokines and CX_3CR1 mRNA expression on the 14th day after mAb 1-22-3 injection with or without treatment of candesartan. mRNA expression was semiquantitated by RT-PCR using cDNA corresponding to 750 ng RNA. The optimal cycle numbers were determined in a preliminary trial to be in the linear phase of amplification. (*A*) The findings of candesartan treated group are shown in the upper panel, and those of the nephritic control without treatment of candesartan (PBS injected group) are in the bottom panel. Representative agarose gel electrophoretic patterns of PCR products of FKN, CX_3CR1, MCP-1, MDC, and GAPDH in 3 cycle intervals are shown. (*B*) Ratios of the densitometric signals of (■) FKN, (▨) CX_3CR1, (□) MCP-1 or (▤) MDC and the internal control (GAPDH) were analyzed. The data are shown as ratio relative to PBS injected group and are expressed as mean ± SD of three independent experiments. Candesatran treatment reduced the expression of FKN and CX_3CR1. By contrast, candesartan treatment increased MCP-1 mRNA expression. (*C*) Real-time RT-PCR analysis of fractalkine in rats treated with candesartan. The x-axis shows the number of PCR cycles, and the y-axis is the difference between measured fluorescence and the baseline. Decreased expression of fractalkine in rats treated with candesartan was confirmed. Lines are: (a) GAPDH, PBS injection; (b) GAPDH candesartan treated; (c) FKN, PBS injection; (d) FKN, candesartan-treated.

We also observed that mRNA expression of CX_3CR1 (Fig. 4) and the number of the recruited CX_3CR1^+ cells in glomeruli were much higher in the uninephrectomized model than in the sham operated model. We confirmed that fractalkine was concerned with the recruitment of leukocytes into glomeruli in mAb 1-22-3-induced nephropathy by the chemotaxis experiment using the leukocytes prepared from glomeruli of rats injected with mAb 1-22-3 (Fig. 7). To analyze whether the expression of fractalkine and CX_3CR1 is the unique finding in the uninephrectomized prolonged model, or if they commonly participate in the development of the prolonged mesangial alterations, the fractalkine expression was investigated in another prolonged model induced by two consecutive injections of mAb 1-22-3 into rats without pre-uninephrectomy. The expressions of fractalkine and CX_3CR1 after the second mAb 1-22-3 injection were much higher than those after the first injection (Fig. 10). Together, these findings suggested that fractalkine expression and the recruitment of CX_3CR1^+ cells play an important role on the development of the prolonged glomerular alterations.

The reason that fractalkine expression is higher in these prolonged models than in the reversible model

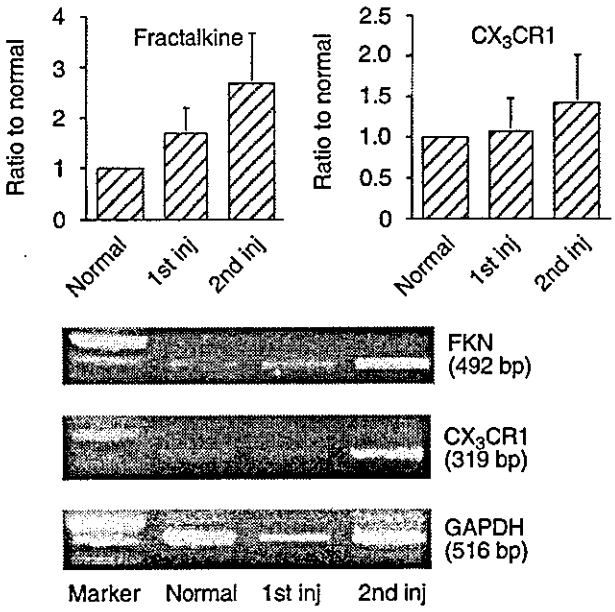

Fig. 10. Fractalkine (FKN) and CX_3CR1 expression on the 14th day after the first and the second mAb 1-22-3 injections. mRNA expression was semiquantitated by RT-PCR using cDNA corresponding to 750 ng RNA. The optimal cycle numbers were determined in a preliminary trial to be in the linear phase of amplification. Ratios of the densitometric signals of FKN or CX_3CR1 and the internal control (GAPDH) were analyzed. The data are shown as ratio relative to normal rat findings and are expressed as mean ± SD of three independent experiments. FKN and CX_3CR1 mRNA expressions after the second mAb injection are higher than those after the first injection.

remains unclear. However, the findings obtained in this study give us a possible clue. Fractalkine is considered to be important for leukocytes recruitment especially in tissue with a high blood flow rate [34, 35], because fractalkine functions as both a chemoattractant and an adhesion molecule for leukocytes [20, 21]. Feng et al reported that fractalkine might play an important role for the recruitment of leukocytes in glomeruli, because glomeruli have a high blood flow rate [22]. Because uninephrectomy causes glomerular hypertension in the remaining kidney, it is conceivable that fractalkine might play a more important role in the remaining kidney of our nephrectomized model. Fractalkine was expressed more actively under the condition with glomerular hypertension for the development of inflammatory responses. In the prolonged model caused by the consecutive injections of mAb 1-22-3, the locally increased blood pressure in the glomeruli—the structure of which was damaged by the first injection of mAb 1-22-3—might be involved in the highly expression of fractalkine. Of course, another possibility cannot be ruled out. Two recent reports have suggested that glomerular hypertension is not essential for the development of prolonged glomerular alterations [36, 37]. Another possibility is that some cytokines act on mesangial cells to produce fractalkine. Whatever the mechanism, we believe that the increased expression of fractalkine in the injured glomeruli contributes to causing the prolonged glomerular alterations.

This study shows that AT1RA treatment ameliorated the glomerular morphological findings at six weeks in the nephrectomized prolonged model, although the treatment did not ameliorate the glomerular morphological findings at two weeks. We clearly demonstrated that the immunostaining and mRNA expression of fractalkine and the number of CX_3CR1^+ cells recruited in glomeruli were already decreased at two weeks after disease induction in rats treated with AT1RA (Figs. 8 and 9). These findings indicate that the expression of fractalkine/CX_3CR1 could be a predictor of the prolonged disease, and suggest that fractalkine/CX_3CR1 contributes to the development of the glomerular alterations. Although the precise therapeutic mechanism of AT1RA on proteinuria and mesangial proliferation remains unclear [38–42], it has been reported that AT1RA ameliorates the glomerular hypertension by relaxing the efferent microartery [42]. AT1RA did not influence the glomerular alterations detected at two weeks after disease induction. The early stage of Thy 1 nephritis is characterized by the mesangiolysis caused by the binding of anti-Thy 1 antibody and the consequent mesangial cell proliferation and the matrix expansion detected at two weeks. It is accepted that these alterations are self-limiting. These glomerular alterations of the early stage were observed similarly in both prolonged and the reversible models. We consider that glomerular hypertension contributes to the development of the prolonged glomerular alterations. It is conceivable that AT1RA prevents the development of the prolonged alterations by reducing the glomerular hypertension. Interestingly, we observed the increased MCP-1 expression in rats treated with AT1RA. Stahl et al reported that MCP-1 is produced by mesangial cell in Thy 1 nephritis [43]. Our current study shows that fractalkine also is produced by mesangial cells. The reason why AT1RA treatment increased the expression of MCP-1 is not clear. However, this might be explained by the following mechanism: In the high shear environment, mesangial cells produce fractalkine more actively than MCP-1. The AT1RA treatment might prevent this alternative response of the mesangial cell, which then would increase the MCP-1 expression.

Using dual-labeled IF studies, the localization of fractalkine was analyzed to determine the exact subpopulations of the leukocyte containing the CX_3CR1^+ cells. Fractalkine was expressed by endothelial cells in the early phase of the uninephrectomized model (Fig. 5D). Interestingly, fractalkine staining was detected not only at the endothelial cells but also in the mesangial area (Fig. 5 E, F) in the later phase of the prolonged model. Dual labeling studies with markers of inflammatory cells

showed that the major parts of the CX_3CR1^+ cells in glomeruli are not T-lymphocytes but macrophages (Fig. 5 G-I and Fig. 6). Our study used two phenotypic markers of macrophages, ED1 and ED3. ED1 is widely used as a pan-monocyte/macrophage marker, and ED3 was originally reported as confined to lymphoid organs [44] but $ED3^+$ cells have been found at sites of immunologically-mediated tissue inflammation in several experimental models [45–48]. Although the precise characteristics of the $ED3^+$ cells has not been clarified, $ED3^+$ cells are reported to be activated macrophages. Our findings showed that 66.7% of CX_3CR1^+ cells in glomeruli were $ED3^+$ cells, and 69.5% of the total $ED3^+$ cells in glomeruli were CX_3CR1^+ cells on the fifth day of the prolonged model. In vitro chemotaxis analysis showed that $ED3^+$ cells in glomeruli in mAb 1-22-3-induced GN could be attracted by fractalkine (Fig. 7D). All of these findings suggest that the $ED3^+/CX_3CR1^+$ cells attracted by fractalkine play important roles for the development of the prolonged glomerular alterations.

In conclusion, immunohistological study and chemotaxis analysis shows that fractalkine is highly concerned with the recruitment of leukocytes into glomeruli in mAb 1-22-3–induced nephritis. Our study demonstrates that the expression of fractalkine and the recruitment of CX_3CR1^+ cells in glomeruli are dominant in the prolonged models of mesangial proliferative GN. Taken together, these findings suggest that the fractalkine/CX_3CR1 might be involved in the development of the prolonged mesangial alterations.

ACKNOWLEDGMENTS

This work was supported by Grant-Aids for Scientific Research (B) (13557084 to H. Kawachi), Grant-Aids for Scientific Research (B) (08457286 to F. Shimizu) from the Ministry of Education, Science, Culture, Sports of Japan, Grant-Aids from Naito Memorial Foundation (to H. Kawachi), and Grant-Aids from Tsukada Medical Foundation (to Y. Ikezumi). The authors express their gratitude to Ms. M. Oba, Ms. Y. Kondo, and Ms. C. Nagasawa for their technical assistance. A portion of this work was presented at the 32nd Annual Meeting of the American Society of Nephrology, Miami, Florida, USA in 1999, and published in abstract form (*J Am Soc Nephrol* 10:529A, 1999).

Reprint requests to Hiroshi Kawachi, M.D., Ph.D., Department of Cell Biology, Institute of Nephrology, Niigata University Graduate School of Medical and Dental Sciences, 1-757 Asahimachi-dori, Niigata 951-8510, Japan.
E-mail: kawachi@med.niigata-u.ac.jp

REFERENCES

1. Nolasco FEB, Cameron JS, Hartley B, *et al*: Intraglomerular T cells and monocytes in nephritis: Study with monoclonal antibodies. *Kidney Int* 31:1160–1166, 1987
2. Hooke DH, Gee DC, Atkins RC: Leukocyte analysis using monoclonal antibodies in human glomerulonephritis. *Kidney Int* 31:964–972, 1987
3. Markovic-Lipkovski J, Müller CA, Risler T, *et al*: Association of glomerular and interstitial mononuclear leukocytes with different forms of glomerulonephritis. *Nephrol Dial Transplant* 5:10–17, 1990
4. Li H, Hancock WW, Hooke DH, *et al*: Mononuclear cell activation and decreased renal function in IgA nephropathy with crescents. *Kidney Int* 37:1552–1556, 1990
5. Li H, Hancock WW, Dowling JP, Atkins RC: Activated ($IL\text{-}2R^+$) intraglomerular mononuclear cells in crescentic glomerulonephritis. *Kidney Int* 39:793–798, 1991
6. Arrizabalaga P, Solé M, Quintó IL, Ascaso C: Intercellular adhesion molecule-1 mediated interactions and leucocyte infiltration in IgA nephropathy. *Nephrol Dial Transplant* 12:2258–2262, 1997
7. Radeke HH, Reach K: The inflammatory function of renal glomerular mesangial cells and their interaction with the cellular immune system. *Clin Invest* 70:825–842, 1992
8. Floege J, Johnson RJ, Couser WG: Mesangial cells in the pathogenesis of progressive glomerular disease in animal models. *Clin Invest* 70:857–864, 1992
9. Cattell V: Macrophages in acute glomerular inflammation. *Kidney Int* 45:945–952, 1994
10. Remuzzi G, Zoja C, Rerico N: Proinflammatory mediators of glomerular injury and mechanisms of activation of autoreactive T cells. *Kidney Int* 45(Suppl 44):S8–S16, 1994
11. Floege J, Grone HJ: Progression of renal failure: What is the role of cytokines? *Nephrol Dial Transplant* 10:1575–1586, 1995
12. Ikezumi Y, Kawachi H, Toyabe S, *et al*: An anti-CD5 monoclonal antibody ameliorates proteinuria and glomerular lesions in rat mesangioproliferative glomerulonephritis. *Kidney Int* 58:21–34, 2000
13. Yamamoto T, Yamamoto K, Kawasaki K, *et al*: Immunoelectron microscopic demonstration of Thy-1 antigen on the surface of mesangial cells in the rat glomerulus. *Nephron* 43:293–298, 1986
14. Yamamoto T, Wilson CB: Quantitative and qualitative studies of antibody-induced mesangial cell damage in the rat. *Kidney Int* 32: 514–525, 1987
15. Border WA, Okuda S, Languino LR, *et al*: Suppression of experimental glomerulonephritis by antiserum against transforming growth factor β1. *Nature* 346:371–374, 1990
16. Johnson RJ, Iida H, Alpers CE, *et al*: Expression of smooth muscle cell phenotype by rat mesangial cells in immune complex nephritis. Alpha-smooth muscle actin is a marker of mesangial cell proliferation. *J Clin Invest* 87:847–858, 1991
17. Nakayama H, Oite T, Kawachi H, *et al*: Comparative nephritogenicity of two monoclonal antibodies that recognize different epitopes of rat Thy-1.1 molecule. *Nephron* 78:453–463, 1998
18. Cheng QL, Orikasa M, Morioka T, *et al*: Progressive renal lesions induced by administration of monoclonal antibody 1-22-3 to uninephrectomized rats. *Clin Exp Immunol* 102:181–185, 1995
19. Weissgarten J, Golik A, Cohn M, *et al*: Nephrectomy enhances interleukin 6 secretion by interleukin 1-stimulated mesangial cells in vitro. *J Nephrol* 11:199–202, 1998
20. Bazan JF, Bacon KB, Hadiman G, *et al*: A new class of membrane-bound chemokine with a CX_3C motif. *Nature* 385:640–644, 1997
21. Fong AM, Robinson LA, Steeber DA, *et al*: Fractalkine and CX_3CR1 mediate a novel mechanism of leukocyte capture, firm adhesion, and activation under physiologic flow. *J Exp Med* 188: 1413–1419, 1998
22. Feng L, Chen S, Garcia GE, *et al*: Prevention of crescentic glomerulonephritis by immunoneutralization of the fractalkine receptor CX_3CR1. *Kidney Int* 56:612–620, 1999
23. Chen S, Bacon KB, Li L, *et al*: In vivo inhibition of CC and CX_3C chemokine-induced leukocyte infiltration and attenuation of glomerulonephritis in Wistar-Kyoto (WKY) rats by vMIP-II. *J Exp Med* 188:193–198, 1998
24. Raij L, Azar S, Keane W: Mesangial injury, hypertension, and progressive glomerular damage in Dahl rats. *Kidney Int* 26:137–143, 1984
25. Johnson RJ, Pritzl P, Iida H, Alpers E: Platelet-complement interactions in mesangial proliferative nephritis in rat. *Am J Pathol* 138:313–321, 1991
26. Floege J, Burg M, Hugo C, *et al*: Endogenous fibroblast growth factor-2 mediates cytotoxicity in experimental mesangioproliferative glomerulonephritis. *J Am Soc Nephrol* 9:792–801, 1998
27. Kawachi H, Oite T, Shimizu F: Quantitative study of mesangial

injury with proteinuria induced by monoclonal antibody 1-22-3. *Clin Exp Immunol* 92:342–346, 1993
28. Natori Yu, Ou ZL, Yamamoto-Shuda Y, Natori Ya: Expression of lymphotactin mRNA in experimental crescentic glomerulonephritis. *Clin Exp Immunol* 113:265–268, 1998
29. Cook HT, Smith J, Cattel V: Isolation and characterization of inflammatory leukocytes from glomeruli in an in situ model of glomerulonephritis in the rat. *Am J Pathol* 126:126–136, 1987
30. Nakamura T, Obata J, Kimura H, *et al*: Blocking angiotensin II ameliorates proteinuria and glomerular lesions in progressive mesangioproliferative glomerulonephritis. *Kidney Int* 55:877–889, 1999
31. Kawachi H, Iwanaga T, Toyabe S, *et al*: Mesangial sclerotic change with persistent proteinuria in rats after two consecutive injections of monoclonal antibody 1-22-3. *Clin Exp Immunol* 90: 129–134, 1992
32. Kawachi H, Orikasa M, Matsui K, *et al*: Epitope-specific induction of mesangial lesions with proteinuria by a moAb against mesangial cell surface antigen. *Clin Exp Immunol* 88:399–404, 1992
33. Oite T, Saito M, Suzuki Y, Arii T, *et al*: A specific Thy1 molecule epitope expressed on rat mesangial cells. *Exp Nephrol* 4:350–360, 1996
34. Mackay CR: Chemokines: What chemokine is that? *Curr Biol* 7: R384–R386, 1997
35. Scahll T: Fractalkine: A strange attractor in the chemokine landscape. *Immunol Today* 18:147, 1997
36. Oyanagi-Tanaka Y, Jian Y, Wada Y, *et al*: Real-time observation of hemodynamic changes in glomerular aneurysms induced by anti-Thy-1 antibody. *Kidney Int* 59: 252–259, 2001
37. Wenzel UO, Wolf G, Thaiss F, *et al*: Renovascular hypertension does not influence repair of glomerular lesions induced by anti-thymocyte glomerulonephritis. *Kidney Int* 58:1135–1147, 2000
38. Remuzzi AR, Perico N, Sangalli F, *et al*: ACE inhibition and ANG II receptor blockade improve glomerular size-selectivity in IgA nephropathy. *Am J Physiol* 276:F457–F466, 1999
39. Perico N, Remuzzi A, Sangalli F, *et al*: The antiproteinuric effect of angiotensin antagonism in human IgA nephropathy is potentiated by indomethacin. *J Am Soc Nephrol* 9:2308–2317, 1998
40. Lafayette RA, Mayer G, Park SK, Meyer TW: Angiotensin II receptor blockade limits glomerular injury in rats with reduced renal mass. *J Clin Invest* 90:766–771, 1992
41. Nakajima M, Hutchinson HG, Fujinaga M, *et al*: The angiotensin II type 2 (AT2) receptor antagonized the growth effects of the AT1 receptor: Gain-of-function study using gene transfer. *Proc Natl Acad Sci USA* 92:10663–10667, 1995
42. Matsuoka T, Hymes J, Ichikawa I: Angiotensin in progressive renal diseases: Theory and practice. *J Am Soc Nephrol* 7:2025–2043, 1996
43. Stahl RAK, Thaiss F, Disser M, *et al*: Increased expression of monocyte chemoattractant protein-1 in anti-thymocyte antibody-induced glomerulonephritis. *Kidney Int* 44:1036–1047, 1993
44. Dijkstra CD, Dopp EA, Joling P, Kraal G: The heterogeneity of mononuclear phagocytes in lymphoid organs: distinct macrophage subpopulations in the rat recognized by monoclonal antibodies ED1, ED2 and ED3. *Immunology* 54:589–599, 1985
45. Kool J, Gerritis-Boeye MY, Severijnen AJ, Hazenberg MP: Immunohistology of joint inflammation induced in rats by cell wall fragments *Eubacterium aerofaciens*. *Scand J Immunol* 36:497–506, 1992
46. Polman CH, Dijkstra CD, SminiaT, Koetsier JC: Immunohistological analysis of macrophages in the central nervous system of Lewis rats with experimental allergic encephalomyelitis. *J Neuroimmunol* 11:215–222, 1986
47. Noble B, Ren K, Taverne J, *et al*: Mononuclear cells in glomeruli and cytokines in urine reflect the severity of experimental proliferative immune complex glomerulonephritis. *Clin Exp Immunol* 80: 281–287, 1990
48. Cook HT, Singh SJ, Wembridge DE, *et al*: Interleukin-4 ameliorates crescentic glomerulonephritis in Wistar Kyoto rats. *Kidney Int* 55:1319–1326, 1999

Kidney International, Vol. 62 (2002), pp. 763–769

Tornado extraction: A method to enrich and purify RNA from the nephrogenic zone of the neonatal rat kidney

TAKAHITO ITO, AKIRA SUZUKI, ENYU IMAI, NAOKO HORIMOTO, TOMOKAZU OHNISHI, YASUSHI DAIKUHARA, and MASATSUGU HORI

Osaka University Graduate School of Medicine, Department of Internal Medicine and Therapeutics, Osaka, and Kagoshima University Dental School, Department of Biochemistry, Kagoshima, Japan

Tornado extraction: A method to enrich and purify RNA from the nephrogenic zone of the neonatal rat kidney.

Background. Development of the kidney is a complicated and tightly regulated process. Although several genes responsible for the renal development have been identified to date, the precise mechanisms of spatial and temporal regulation remain to be elucidated. Therefore, expanding our knowledge of molecules that are associated with nephrogenesis will be helpful to understand the whole process.

Methods. To extract RNA selectively from the nephrogenic zone of the developing kidney, we developed a simple and reliable method.

Results. This method, named "tornado extraction," enriched RNA of the nephrogenic zone by about 30-fold. In combination with the suppression subtractive hybridization, a considerable number of genes that were differentially expressed in the nephrogenic zone were obtained. These genes included a series of endodermal markers such as albumin and α-fetoprotein as well as GDNF (glia-derived neurotrophic factor), osteoblast-specific factor-2 (OSF-2)/periostin and fetuin (one of the major serum proteins in the fetus).

Conclusion. Tornado extraction has great value in studying genes in the nephrogenic zone of the developing kidney. Since the quality of RNA obtained by this method is excellent, tornado extraction is suitable in combination with other techniques including the subtractive hybridization method and DNA microarray analysis.

Development of the kidney has been extensively studied as a model of organogenesis and vasculogenesis. These studies were achieved by using morphological analysis, microsurgery, in vitro cultivation, microchemistry, targeted mutation and other transgenic technologies [1–3]. To date, a number of genes that are indispensable for the nephrogenesis have been identified including transcription factors, adhesion molecules, growth factors and their receptors. Nevertheless, the development of the kidney is highly sophisticated and under strict controls of the differentiation and spatial assembly of several cell lineages. Our knowledge base in understanding the entire framework of nephrogenesis is still small, which prompted us to explore further for genes using other strategies.

In contrast to human newborns, the kidney of neonatal rats is still under structural development. In the cortical nephrogenic zone, nephrons are in early stages of the development showing primitive structures such as the mesenchymal condensation and the comma-shaped bodies that are surrounded by immature mesenchymal cells [4]. Glomerular components including endothelial cells and mesangial cells are being integrated into immature nephrons at the capillary-loop stage, while tubules and collecting ducts are also under growth and differentiation in order to accommodate further development of the kidney size [4, 5]. Therefore, searching genes that are exclusively expressed in the nephrogenic zone is an intriguing issue to further understand the mechanism of the nephrogenesis.

To discover candidate genes that may be relevant to the nephrogenesis, we decided to identify genes that are differentially expressed in the nephrogenic zone of the neonatal rat kidney in comparison with the adult rat kidney, because temporal up-regulation of genes suggests that they may actively contribute to the development of the kidney. Alternatively, such genes may be useful as markers to define cellular lineages or developmental stages.

In the present study, we developed a new RNA extraction method named "tornado extraction" in order to extract RNA selectively from the nephrogenic zone of the neonatal rat kidney. Efficiency of the enrichment was estimated at about 30-fold. This method allowed the purification of a sufficient amount of RNA from the nephrogenic zone of the kidney without using any tedious micro-dissection techniques. Importantly, the quality of

Key words: nephrogenesis, subtractive hybridization, microarray, embryonic kidney, renal development.

Received for publication August 28, 2001
and in revised form April 1, 2002
Accepted for publication April 22, 2002

RNA obtained by tornado extraction from the nephrogenic zone was sufficiently excellent to provide poly $(A)^+$ RNA of high quality. We analyzed differentially expressed genes in the nephrogenic zone in combination with the suppression subtractive hybridization analysis (SSH), a method that is composed of normalization (self-subtraction), subtraction and polymerase chain reaction (PCR) [6]. Within the limited number of sequences in our studies, a number of genes were identified, such as albumin, α-fetoprotein, transferrin, inter-alpha-trypsin inhibitor and fibrinogen, which are thought to be definitive endodermal markers [7, 8]. We also found that OSF-2/periostin was rich in the nephrogenic zone. Thus, tornado extraction is a useful tool to study transcripts in the nephrogenic zone.

METHODS

Animals

One-day-old and six-week-old Sprague-Dawley (SD) rats were used. Rats were anesthetized by intraperitoneal administration of pentobarbital. Then the kidneys were removed surgically and immediately dipped in liquid nitrogen to freeze. All procedures were approved by the Osaka University School of Medicine Animal Committee.

RNA extraction

One by one, kidneys were obtained from one-day-old SD rats and were stored in liquid nitrogen until 60 kidneys were collected and stored. Then, the frozen kidneys were transferred into a fresh 50-mL conical tube that was filled with liquid nitrogen. During this step, the tube was held in a jar filled with liquid nitrogen to prevent accidental activation of RNase. The tube into which all kidneys were transferred was left at room temperature to evaporate the liquid nitrogen, and the tube was gently swirled in order to prevent aggregation of kidneys. Once the liquid nitrogen evaporated completely, 30 mL of RNA extraction buffer (Trizol™; Life Technology, Paisley, UK) were added. Immediately, the tube was vortexed at the maximum speed for 20 seconds at room temperature, and the extraction buffer was quickly transferred to a fresh tube by decantation. Plenty of the buffer at room temperature was used to avoid freezing the buffer when it was mixed with frozen kidneys in the tube. Finally, RNA in the extraction buffer was purified according to the manufacturer's instruction. Poly $(A)^+$ RNA was prepared with the Oligotex mRNA purification kit (Takara, Shiga, Japan). Another set of RNA was purified from whole kidneys of three neonatal or adult rats as well.

Suppression subtractive hybridization and cDNA sequencing

Suppression subtractive hybridization (SSH) was carried between two Poly $(A)^+$ RNA sets using the PCR-SELECT system (Clontech, Palo Alto, CA, USA) according to the manufacturer's instructions. All synthesized cDNA sets were cut with a 4-base cutter, *Rsa*I, and were ligated to the adaptors supplied in the kit. Thermal cycling was performed as described in the manufacturer's instructions except for the cycling number. The subtracted cDNA pools were amplified by the combination of 30 cycles at the first PCR and 14 cycles at the second nested PCR. The final SSH products from the nephrogenic zone-enriched cDNA pool were separated in 2% agarose gel electrophoresis, and the products over 100 bp were extracted from the gel. The recovered sequences were ligated to pSTBlue-1 plasmid vectors (Novagen, Madison, WI, USA). The resultant nephrogenic zone-enriched cDNA library was introduced into *E. coli* DH5α, and plated onto LB agar plates containing 100 μg/mL of ampicillin. Anonymously chosen clones were subjected to cDNA sequencing by using Big Dye terminator cycle sequencing system on an ABI Prism 310 DNA sequencer (Applied Biosystems, Foster City, CA, USA). BLAST was used for searching existing databases.

Northern blot analysis and in situ hybridization

Fifteen micrograms of RNA per lane were electrophoresed through 1.5% agarose/2% formaldehyde gel, were transferred onto nylon membrane and were fixed to the membrane with UV. The membrane was hybridized at 42°C overnight with radioactively labeled cDNA fragments, and were washed twice in 2× standard sodium citrate (SSC)/0.1% sodium dodecyl sulfate (SDS) at room temperature, then twice in 0.1× SSC/0.1% SDS at 65°C. The membrane was then exposed to Kodak X-AR film (Kodak, Rochester, NY, USA). For in situ hybridization, rats were anesthetized and perfused. Tissues were fixed with 4% paraformaldehyde at 4°C for six hours and were embedded in paraffin. Four-micrometer-thick paraffin sections were hybridized with cRNA probes. The cRNA probes were labeled with digoxigenin and detected by a digoxigenin detection system (Boehringer Mannheim GmbH, Mannheim, Germany) according to the manufacturer's instruction. The sections were stained with methyl green to visualize the nuclei.

Immunohistochemistry

Paraffin-embedded tissues also were subjected to immunohistochemistry. Four-micrometer thick sections were stained with mouse anti-fetuin monoclonal antibody that was described previously [9]. Signals were visualized by the ABC kit (Vector Laboratories, Burlingame, CA, USA). The sections were observed under a microscope (Eclipse E600; Nikon, Tokyo, Japan), and all images were captured by a digital imaging system.

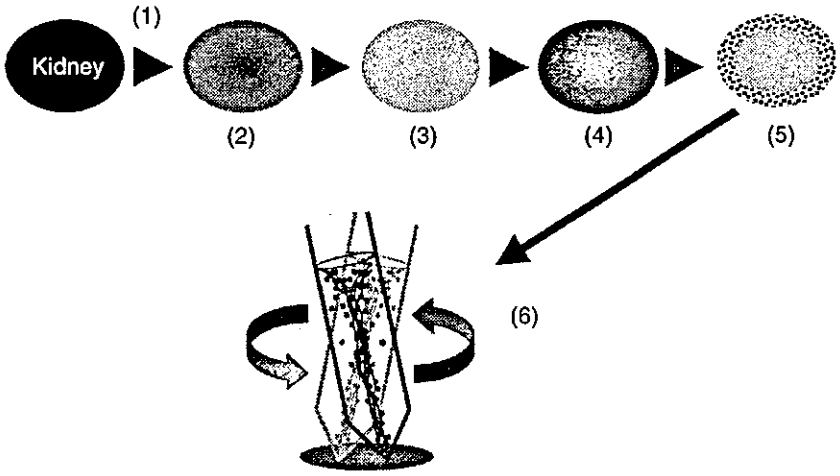

Fig. 1. Schematic of the tornado extraction method. The frozen part of the kidney is designated by the gray color. (*1*) Kidneys are dipped into liquid nitrogen. (*2*) Kidneys start freezing from the subcapsular region. (*3*) Kidneys totally freeze. (*4–5*) Kidneys begin thawing from the subcapsular region in the RNA extraction buffer. (*6*) Vortex facilitates extracting RNA from the thawing subcapsular region.

RESULTS AND DISCUSSION

To identify genes specific to the nephrogenic zone, which is composed of the mesenchymal stroma and the immature nephron such as the mesenchymal condensation, the comma-shaped body, the S-shaped body and the tip of the branching ureteric bud, we established the new tornado extraction method. Tornado extraction allowed us to extract RNA selectively from the subcapsular nephrogenic zone of the developing kidney. This technique does not require any special equipment, is very easy to follow, and no special skill is needed to perform the process.

The theoretical background for the tornado extraction technique is very simple (Fig. 1). During the procedure, RNA in the subcapsular region is free from RNase because the surface freezes quickly in liquid nitrogen. RNA extraction buffer lyses only the subcapsular region of frozen kidneys because it takes more time for the core of frozen kidneys to thaw and to contact with the extraction buffer. Vigorous vortexing helps the efficient and uniform extraction of RNA from the cortical nephrogenic zone. Tornado extraction is named after the swirling extraction buffer. From 60 neonatal rat kidneys, an average of 400 μg of RNA was obtained, while one whole kidney at this age contained about 200 μg of RNA. Therefore, RNA in the cortical nephrogenic zone was enriched approximately by 30-fold. Since quality and quantity of RNA obtained by this method is excellent and its procedure is quite simple, we believe that tornado extraction is the best method to purify RNA from the nephrogenic zone of the developing kidney.

Subsequently, we attempted to find genes that were differentially expressed in the nephrogenic zone by using a combination of the tornado extraction and SSH methods. Glia-derived neurotrophic factor (GDNF) was identified in the first round sequencing of anonymously selected clones. GDNF that is secreted from the tip of the branching ureteric bud plays an indispensable role in nephrogenesis [10]. While GDNF was easily identified in the present study, it did not come up as a differentially expressed gene in our previous analysis of 200 clones collected by SSH using the whole kidney of neonatal rats as the tester (our unpublished results). Presumably this was because the expression of GDNF was highly restricted to the tips of the ureteric bud, which were scattered only in the nephrogenic zone. Our result also showed that a series of endodermal markers such as albumin, α-fetoprotein, transferrin, inter-α-trypsin inhibitor, and fibrinogen were expressed in the developing nephron (albumin and inter-α-trypsin inhibitor are shown in Figs. 2 and 5, respectively). Again, these genes were never identified in our previous attempt, where the tester RNA was extracted from the whole kidney of neonates (data not shown). In other words, it is obvious that the tornado extraction method of the neonatal kidney efficiently enriched the RNA of the nephrogenic zone, and that the combination of tornado extraction and SSH greatly aided the identification of genes specific to the nephrogenic zone.

More than 10 years ago the existence of endoderm-specific genes such as albumin and α-fetoprotein was found in the developing nephron independently [11–14]. Albumin and α-fetoprotein also are expressed in lung and heart of fetuses or neonates [11, 15, 16]. At least in the case of albumin and α-fetoprotein, both of which are adjacently located on chromosome 4 in human, 14 in rat, and 5 in mouse, it seems that hepatocyte nuclear factor 1 (HNF1), a transcription factor, seems to play a fundamental role for the expression of both genes in the developing nephron. HNF1, when mutated, is responsible for maturity-onset diabetes of the young-3 (MODY3) [17]. Deletion of the HNF1 binding site from the albumin

promoter removes almost all promoter activity in the presence or absence of enhancers, whereas the site itself contributes little to direct stimulation of the transcription [18]. Homozygous HNF1-deficient mice suffered from renal tubular dysfunction [19], which implies a role for HNF1 in renal development. However, the roles of albumin and α-fetoprotein in renal development are still enigmatic. It is noteworthy that the existence of these endoderm-specific genes does not present any consistent relationship with embryonic origin, although the expression of these genes is often referred to as evidence of endodermal derivation or sometimes as proof of hepatocytes in vivo and in vitro [7, 8]. At the very least, unusual expression of these genes can be used to define the developmental stage of the nephron.

Messenger RNA of fetuin/α_2-HS-glycoprotein, a fetal plasma protein synthesized mainly in liver, also was identified in the developing nephron (Fig. 2). Localization of fetuin mRNA was highly restricted to the nephrogenic zone of the neonatal kidney (Fig. 3A), while fetuin protein product was localized to more mature nephrons and collecting tubules (Fig. 3B). It is known that fetuin is expressed in a wide range of tissues including fetal kidney [20, 21]. Despite its abundance and widespread occurrence, the function remains unknown. Recently, it has been reported that fetuin modifies the function of transforming growth factor-β (TGF-β), bone morphogenic protein (BMP) and hepatocyte growth factor (HGF) in vitro [22, 23]. Since all of these cytokines are relevant in the nephrogenesis, fetuin may play a pivotal role in the nephrogenesis by regulating these factors. The temporal expression pattern of fetuin mRNA in the developing kidney displayed a transient increase 2 days after birth (Fig. 4), which is reminiscent of reports that the expression level of fetuin mRNA fluctuates significantly according to the developmental stage [20, 21, 24].

Among the genes identified in this study, osteoblast-specific factor 2 (OSF-2)/periostin is a unique gene [25]. Originally, OSF-2/periostin was cloned from a mouse osteoblastic cell line [25]. OSF-2/periostin mRNA, whose protein product has a signal sequence without any transmembrane regions, is expressed in bone and to a lesser extent in lung, but not in other tissues including kidney [25]. Because of homology to insect fasciclin I, OSF-2/periostin might function as a homophilic adhesion molecule in bone formation [25]. Our rat 300 bp sequence showed over 90% homology against mouse and human OSF-2/periostin, and therefore it was concluded as rat OSF-2/periostin. In the kidney, OSF-2/periostin mRNA was identified only in RNA of the subcapsular region that was obtained by the tornado extraction method, and not in RNA of the whole kidney when the Northern blot membrane was exposed to a film overnight. A one-week exposure showed the signal in the whole kidney (Fig. 2). In contrast to other genes shown in Figure 2, OSF-2/periostin was not expressed in liver; OSF-2/periostin was more consistently expressed in the kidney during nephrogenesis (Fig. 4). However, in situ hybridization to locate the expression of OSF2/periostin in the neonatal kidney has not worked thus far. Therefore, it is possible that the identification of OSF2/periostin might come

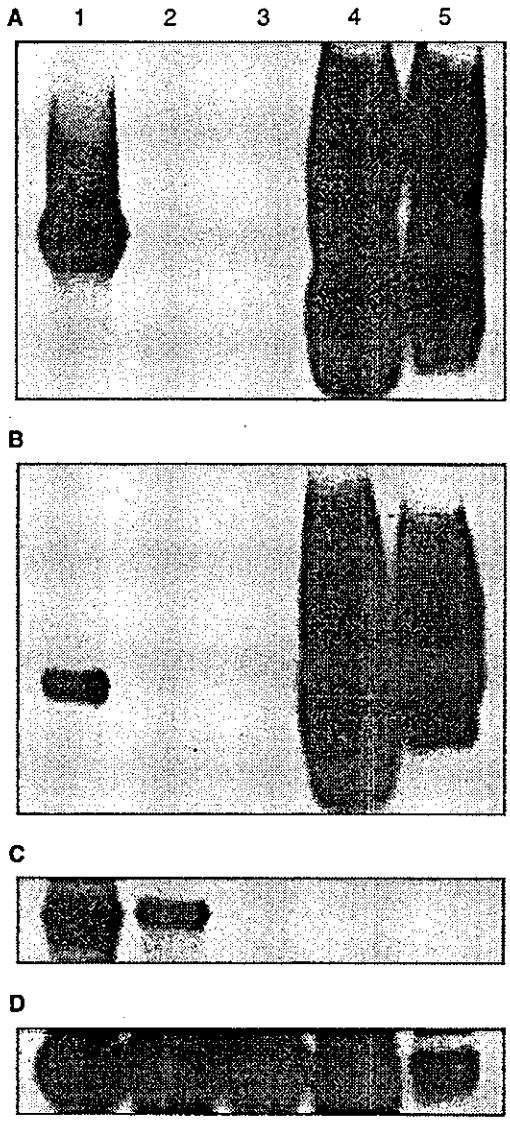

Fig. 2. Northern blot analysis of the differentially expressed genes. Fifteen micrograms of RNA was used for the Northern blot analysis. The filter was exposed to a film at −70°C. (*A*) albumin; (*B*) fetuin/α_2-HS-glycoprotein; (*C*) OSF-2/periostin; (*D*) GAPDH. Panels A, B and D are from an overnight exposure, and panel C is a one week exposure. (Lane 1) RNA obtained from the nephrogenic zone of 1-day-old rat kidneys by tornado extraction; (lane 2) RNA obtained from whole kidneys of 1-day-old rats; (lane 3) RNA obtained from whole kidneys of 6-week-old rats; (lane 4) RNA obtained from liver of 1-day-old rats; (lane 5) RNA obtained from liver of 6-week-old rats. To make the probes, a 400 bp *RsaI-HindIII* fragment of rat albumin cDNA, a 200 bp *PstI-RsaI* fragment of rat fetuin cDNA, and a 300 bp of rat OSF-2/periostin cDNA were used as the templates for making the probes.

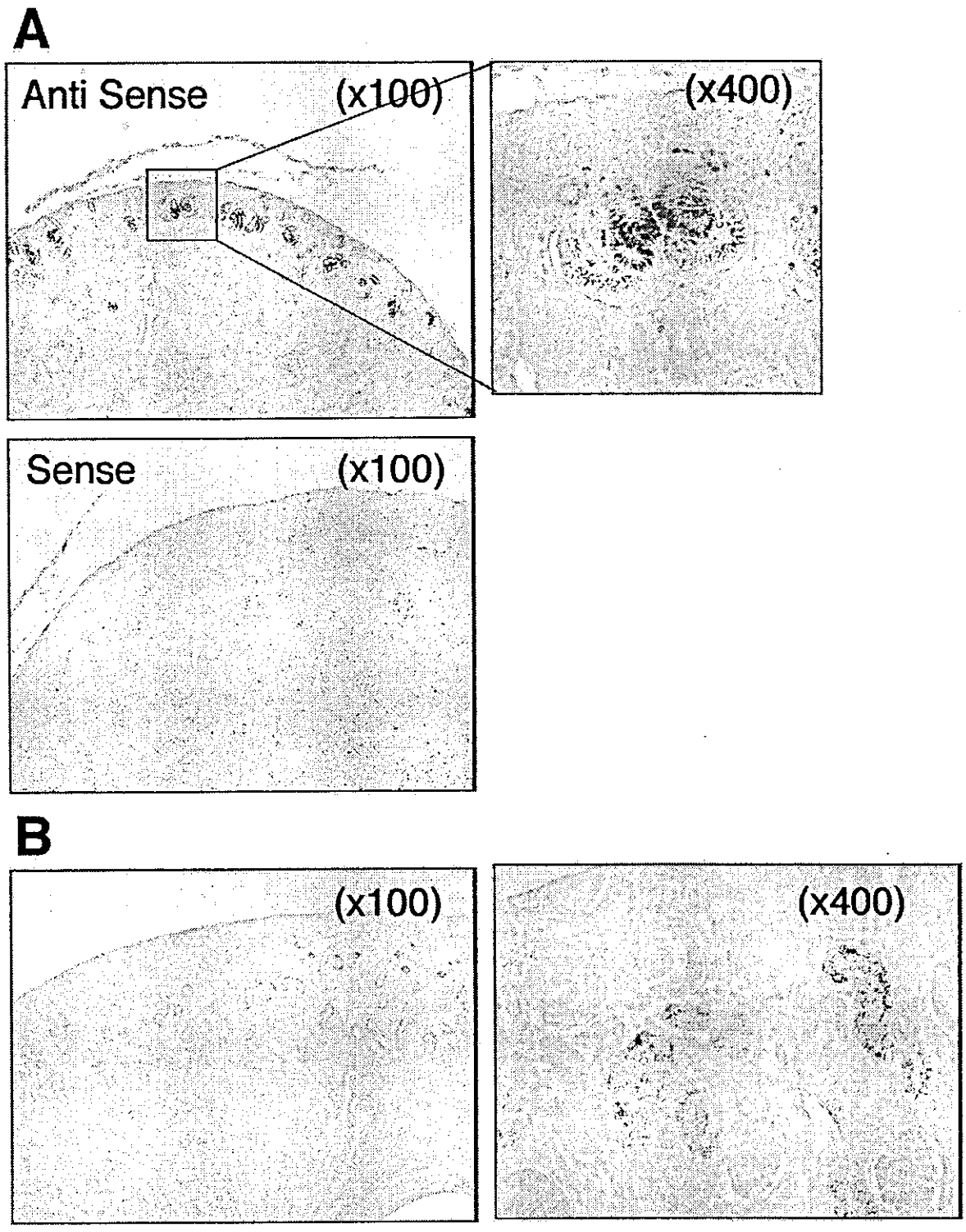

Fig. 3. (*A*) Rat fetuin is expressed in the developing nephron of a one-day-old rat kidney. A digoxigenin-labeled cRNA probe was made. A 200 bp *PstI-RsaI* fragment of rat fetuin cDNA was subcloned into *PstI-SmaI* cut pGEM-3Z vector (Promega), and was used as the template for making the cRNA probe. In situ hybridization analysis revealed that rat fetuin was expressed mainly in the developing nephron, such as the comma-shaped body and the S-shaped body. Glomeruli, ureteric bud and vascular components do not express fetuin. The sections were counterstained with methyl green. (*B*) Immunohistochemical analysis of rat fetuin protein in the 1-day-old rat kidney. Paraffin sections were incubated with anti-rat fetuin monoclonal antibody, then with anti-mouse immunoglobulin antibody. Fetuin protein products are only seen in tubules in the medulla. The sections were counterstained with methyl green.

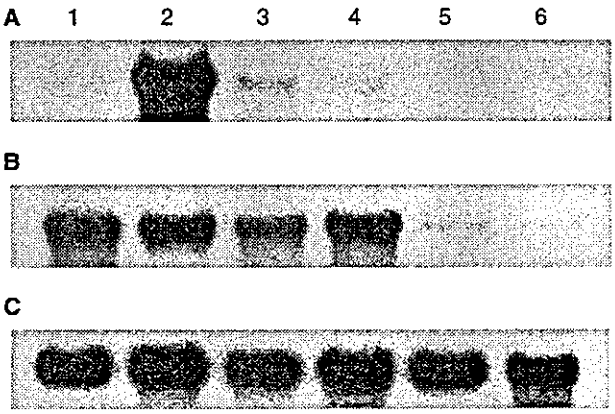

Fig. 4. Temporal expression pattern of fetuin and OSF-2/periostin mRNA. The temporal expression pattern of fetuin and OSF-2/periostin mRNA in the developing kidney was analyzed using Northern blot analysis. A 200 bp *PstI-RsaI* fragment of rat fetuin cDNA and a 300 bp rat OSF-2/periostin cDNA were used as the templates for making the probes. (*A*) fetuin (overnight exposure); (*B*) OSF-2/periostin (1 week exposure); (*C*) GAPDH as the control (overnight exposure). (Lane 1), 1-day-old rat whole kidney; (lane 2), 2-day-old rat whole kidney; (lane 3), 5-day-old rat whole kidney; (lane 4), 10-day-old rat whole kidney; (lane 5), 20-day-old rat whole kidney; (lane 6), 6-week-old rat whole kidney.

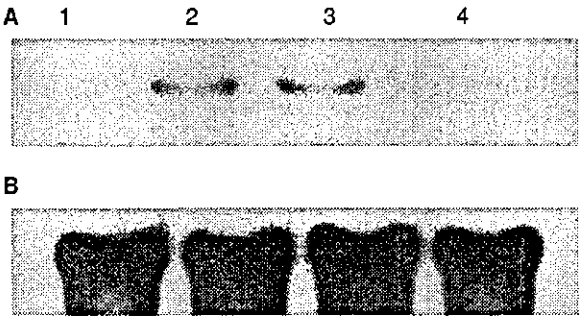

Fig. 5. Expression of inter-α-trypsin inhibitor heavy chain 3 in RNA obtained by tornado extraction. Fifteen micrograms of RNA was used for the Northern blot analysis. The filter was exposed to a film at −70°C overnight. (*A*), inter-α-trypsin inhibitor; (*B*), GAPDH. (Lane 1) RNA obtained from the nephrogenic zone of 1-day-old rat kidneys by tornado extraction; (lane 2) RNA obtained from whole kidneys of 1-day-old rats; (lane 3) RNA obtained from whole kidneys of 6-week-old rats. An 890 bp *RsaI-RsaI* fragment of rat inter-α-trypsin inhibitor cDNA was used as the template for making the probes.

from the difference of cellular composition in the neonatal kidney and the adult kidney: the neonatal kidney might be rich in a type of cells expressing OSF2/periostin, which might be sparsely scattered in the adult kidney.

The expression of inter-α-trypsin inhibitor protein was observed in the proximal tubule of adult rats [26], although its mRNA was originally cloned from liver [27]. Messenger RNA of inter-alpha-trypsin inhibitor heavy chain 3 was rich in the nephrogenic zone of the neonatal rat kidney (Fig. 5).

Sequences that may be relevant to the nephrogenesis or the elongation of tubular epithelium also were obtained. Polypyrimidine tract-binding protein (PTB)-associated splicing factor binds the polypyrimidine tract of mammalian introns and splices pre-mRNA [28]. Macrophage-activation gene-2 is an interferon-γ–inducible gene [29]. Mac-MARKS [30] and cellubrevin [31] are related to vesicle transport. The identification of HSPC-036, which is a chaperone cloned from hematopoietic stem cells, might simply reflect the contamination of $CD34^+$ hematopoietic cells, but is potentially intriguing because these might come from hemangioblasts that produce endothelial cells.

Our attempt provides valuable information, although the number of genes subjected to sequencing was limited. Even in the absence of functional information, genes identified by this approach can be used as differentiation markers in culture experiments such as in vitro differentiation of embryonic stem (ES) cells, or as markers of the tubular epithelium regenerating after injury. Alternatively, some of genes might be useful as tumor markers because developmentally regulated genes are sometimes up-regulated during oncogenesis [32]. In fact, there is a type of renal carcinoma secreting α-fetoprotein [33, 34].

Since the quality of RNA obtained by this method is excellent, tornado extraction is suitable in combination with other techniques including the DNA microarray analysis, and further studies are currently under way.

ACKNOWLEDGMENTS

This research was supported by a Grant-in-Aid for Scientific Research from the Ministry of Education, Science and Culture, Japan, by a grant from Takeda Medical Research Foundation, and by a grant from the Osaka Kidney Foundation (OKF01-0009).

Reprint requests to Takahito Ito, M.D., Department of Internal Medicine and Therapeutics, Osaka University Graduate School of Medicine, 2-2 Yamadaoka, Box A8, Suita, Osaka 565-0871, Japan.
E-mail: taka@medone.med.osaka-u.ac.jp

REFERENCES

1. Bonaldo MF, Lennon G, Soares MB: Normalization and subtraction: Two approach to facilitate gene discovery. *Genome Res* 6:791–806, 1996
2. Vainio S, Muller U: Inductive tissue interactions, cell signaling, and the control of kidney organization. *Cell* 90:975–978, 1997
3. Saxen L: What is needed for kidney differentiation and how do we find it? *Int J Dev Biol* 43:377–380, 1999
4. Saxen L: *Developmental and Cell Biology Series.* New York, Cambridge, Cambridge University Press, 1987
5. Sariola H: Mechanisms and regulation of the vascular growth during kidney differentiation. *Iss Biomed* 14:69–80, 1991
6. Diatchenko L, Lau YFC, Campbell AP, *et al*: Suppression subtractive hybridization: A method for generating differentially regulated or tissue-specific cDNA probes and libraries. *Proc Natl Acad Sci USA* 93:6025–6030, 1996
7. Schuldiner M, Yanuka O, Itskovitz-Eldor J, *et al*: Effects of eight growth factors on the differentiation of cells derived from human embryonic stem cells. *Proc Natl Acad Sci USA* 97:11307–11312, 2000
8. Gualdi R, Bossard P, Zheng M, *et al*: Hepatic specification of the gut endoderm in vitro: Cell signaling and transcriptional control. *Genes Dev* 10:1670–1682, 1996

9. Ohnishi T, Araraki N, Nakamura O, *et al*: Purification, characterization, and studies on biosynthesis of a 59-kDa bone sialic acid-containing protein (BSP) from rat mandible using a monoclonal antibody. *J Biol Chem* 266:14636–14645, 1991
10. Robertson K, Mason I: The GDNF-RET signalling partnership. *Trends Genet* 13:1–3, 1997
11. Nahon JL, Tratner I, Poliard A, *et al*: Albumin and α-fetoprotein gene expression in various nonhepatic rat tissues. *J Biol Chem* 263:11436–11442, 1988
12. Idzerda RL, Behringer RR, Theisen M, *et al*: Expression from the transferrin gene promoter in transgenic mice. *Mol Cell Biol* 9:5154–5162, 1989
13. Levin MJ, Tuil D, Uzan G, *et al*: Expression of the transferrin gene during development of non-hepatic tissues. *Biochem Biophys Res Commun* 122:212–217, 1984
14. Selten GC, Princen HM, Selten-Versteegen AM, *et al*: Sequence content of alpha-fetoprotein, albumin and fibrinogen polypeptide mRNAs in different organs, developing tissues and in liver during carcinogenesis in rats. *Biochim Biophys Acta* 699:131–137, 1982
15. Cote GJ, Chiu JF: Tissue specific control of alpha-fetoprotein gene expression. *Biochem Biophys Res Commun* 120:677–685, 1984
16. Sell S, Longley MA, Boulter J: alpha-Fetoprotein and albumin gene expression in brain and other tissues of fetal and adult rats. *Brain Res* 354:49–53, 1985
17. Yamagata K, Oda N, Kaisaki PJ, *et al*: Mutations in the hepatocyte nuclear factor-1alpha gene in maturity-onset diabetes of the young (MODY3). *Nature* 384:455–457, 1996
18. Vorachek WR, Steppan CM, Lima M, *et al*: Distant enhancers stimulate the albumin promoter through complex proximal binding sites. *J Biol Chem* 275:29031–29041, 2000
19. Pontoglio M, Barra J, Hadchouel M, *et al*: Hepatocyte nuclear factor 1 inactivation results in hepatic dysfunction, phenylketonuria, and renal Fanconi syndrome. *Cell* 84:575–585, 1996
20. Terkelsen OBF, Jahnen-Dechent W, Nielsen H, *et al*: Rat fetuin: Distribution of protein and mRNA in embryonic and neonatal rat tissues. *Anat Embryol (Berl)* 197:125–133, 1998
21. Yang F, Chen ZL, Bergeron JM, *et al*: Human alpha2-HS-glycoprotein/bovine fetuin homologue in mice: Identification and developmental regulation of the gene. *Biochim Biophys Acta* 1130:149–156, 1992
22. Binkert C, Demetriou M, Sukhu B, *et al*: Regulation of osteogenesis by fetuin. *J Biol Chem* 274:28514–28520, 1999
23. Ohnishi T, Nakamura O, Arakaki N, Daikuhara Y: Effect of phosphorylated rat fetuin on the growth of hepatocytes in primary culture in the presence of human hepatocyte growth factor: Evidence that phosphorylated fetuin is a natural modulator of hepatocyte growth factor. *Eur J Biochem* 243:753–761, 1997
24. Kazi JA, Nakamura O, Ohnishi T, *et al*: Changes with age of the rat fetuin concentration in serum and its mRNA expression. *J Biochem (Tokyo)* 124:179–186, 1998
25. Takeshita S, Kikuno R, Tezuka K, Amann E: Osteoblast-specific factor 2: Cloning of a putative bone adhesion protein with homology with the insect protein fasciclin I. *Biochem J* 294:271–278, 1993
26. Moriyama MT, Glenton PA, Khan SR: Expression of inter-alpha inhibitor related proteins in kidneys and urine of hyperoxaluric rats. *J Urol* 165:1687–1692, 2001
27. Chan P, Risler JL, Ranguenez G, Salier JP: The three heavy-chain precursors for the inter-alpha-inhibitor family in mouse: New members of the multicopper oxidase protein group with differential transcription in liver and brain. *Biochem J* 306:505–512, 1995
28. Patton JG, Porro EB, Galceran J, *et al*: Cloning and characterization of PSF, a novel pre-mRNA splicing factor. *Genes Dev* 7:393–406, 1993
29. Wynn TA, Nicolet CM, Paulnock DM: Identification and characterization of a new gene family induced during macrophage activation. *J Immunol* 147:4384–4392, 1991
30. Radau B, Otto A, Muller EC, Westermann P: Protein kinase C alpha-dependent phosphorylation of Golgi proteins. *Electrophoresis* 21:2684–2687, 2000
31. McMahon HT, Ushkaryov YA, Edelmann L, *et al*: Cellubrevin is a ubiquitous tetanus-toxin substrate homologous to a putative synaptic vesicle fusion protein. *Nature* 364:287–289, 1993
32. Davies JA, Perera AD, Walker CL: Mechanisms of epithelial development and neoplasia in the metanephric kidney. *Int J Dev Biol* 43:473–478, 1999
33. Morimoto H, Tanigawa N, Inoue H, *et al*: Alpha-fetoprotein-producing renal cell carcinoma. *Cancer* 61:84–88, 1988
34. Minamoto T, Kitagawa M, Amano N, *et al*: Renal cell carcinoma producing alpha-fetoprotein (AFP) with a unique lectins-affinity profile. *J Surg Oncol* 55:215–221, 1994

Kidney International, Vol. 62 (2002), pp. 780–789

Glucocorticoid regulation of proteoglycan synthesis in mesangial cells

MARI KURODA, HIROYUKI SASAMURA, RYOKO SHIMIZU-HIROTA, MIZUO MIFUNE, HIDEAKI NAKAYA, EMI KOBAYASHI, MATSUHIKO HAYASHI, and TAKAO SARUTA

Department of Internal Medicine, School of Medicine, Keio University, Tokyo, Japan

Glucocorticoid regulation of proteoglycan synthesis in mesangial cells.

Background. Proteoglycans are integral components of the mesangial matrix and glomerular permeability barrier. Recent studies have shown that changes in glomerular proteoglycan expression may play a major role in the pathogenesis of renal disease. Steroid hormones are used as first-choice therapy for the treatment of glomerular diseases, however, the effects of glucocorticoids on expression of glomerular proteoglycans are unknown.

Methods. This study examined the effects of in vitro and in vivo administration of dexamethasone on proteoglycan synthesis and gene expression of proteoglycan core proteins using rat (RMC) and human (HMC) mesangial cells.

Results. Treatment of cultured RMC with dexamethasone resulted in a dose- and time-dependent decrease ($P < 0.05$) in both cell-associated and secreted proteoglycan synthesis to approximately 50% of control levels. This effect was inhibited by the glucocorticoid antagonist mifepristone, and mimicked by prednisolone or corticosterone treatment. Separation of proteoglycans by ion-exchange and gel permeation chromatography suggested that chondrotin sulfate/dermatan sulfate proteoglycans were down-regulated after steroid treatment. Northern blot analysis, RT-PCR, Western blot, and promoter activity assays revealed that dexamethasone caused a significant decrease in decorin mRNA (to 61 ± 8% of controls), whereas biglycan expression and promoter activity were increased after steroid treatment. A similar trend was found in glomeruli isolated from rats treated in vivo with dexamethasone.

Conclusions. These results demonstrate that treatment of mesangial cells with steroids results in a decrease in total proteoglycan synthesis, as well as subtype-specific changes in proteoglycan core protein gene expression by transcriptional control, furthering our understanding of the effects of steroid treatment on the renal glomeruli.

Key words: decorin, biglycan, mesangial matrix, glomerular permeability barrier, steroid hormones, dexamethasone, proteoglycans core protein gene.

Received for publication November 27, 2001
and in revised form April 17, 2002
Accepted for publication April 19, 2002

Glomerular disease is known to be associated with widespread changes in the amount and composition of the mesangial matrix. The major components of this extracellular matrix include collagens, proteoglycans, and fibronectin, which together with numerous less abundant proteins and glycoproteins fulfill a variety of physiological functions in the normal glomerulus.

Proteoglycans are an integral component of this extracellular matrix. These macromolecules have a common structure, consisting of a core protein linked to one or more glycosaminoglycan (GAG) side chains. Due to their structural features, in particular the strong negative charge carried by the GAG moiety, proteoglycans have many unique functions. These include the ability to bind to an array of other molecules such as growth factors, cytokines, enzymes, enzyme inhibitors, and cellular receptors, and to regulate their function [1]. Consequently, the proteoglycan-rich extracellular matrix serves as both a reservoir and a modulator of the actions of a variety of signaling and differentiation factors. In addition, proteoglycans play a direct role in controlling cell growth and differentiation, in modifying cell adhesion, migration and development, and in influencing the deposition of other extracellular matrix components such as collagen. Of interest, the proteoglycans perlecan and agrin also play a major role in forming the glomerular basement membrane negative charge barrier that prevents proteinuria [2].

Based on the composition of the GAG side chains, the proteoglycans may be classified biochemically into chondroitin sulfate (CSPG), dermatan sulfate (DSPG), and heparan sulfate proteoglycans (HSPG). A fourth group of proteoglycans, the keratan sulfate proteoglycans (KSPG) are not highly expressed in the kidney. More recently, the use of molecular cloning techniques has revealed the structure of the major core proteins, resulting in a parallel classification based on the core protein moiety. It is known that the mesangial cell is a major source of the proteoglycans found in the renal glomeruli, and that these cells produce the CSPG versican, the CS/DSPGs biglycan and decorin, as well as the HSPG perlecan [3].

Recent reports have shown that changes in proteoglycan expression may play a crucial role in the pathogenesis of renal disease. It has been shown that dramatic changes in expression of glomerular proteoglycans are characteristic of a variety of renal diseases in humans, including primary glomerulonephritis, diabetic nephrosclerosis, hypertensive nephrosclerosis, and amyloidosis [4–8]. Human studies also have shown that expression of proteoglycans correlates with loss of renal function, suggesting an important pathophysiological role for these glycoproteins in the progression of renal failure [9]. These clinical findings provide support for the evidence from laboratory studies that proteoglycans are involved in events that control matrix expansion and cell proliferation, which are the ultimate features of glomerular sclerosis and renal failure.

Glucocorticoids are widely prescribed for the therapy of glomerulonephritis, and are known to be effective both for the treatment of proteinuria and for the attenuation of the progression of renal failure [10]. However, they are not effective for all forms of renal disease, and the mechanisms of actions of glucocorticoids in ameliorating glomerular disease are still undefined. Despite the widespread use of glucocorticoid therapy for the treatment of renal disease, the effects of glucocorticoids on the expression of renal proteoglycans are unknown. Therefore, the aim of this study was to examine the effects of dexamethasone on proteoglycan production by mesangial cells, to correlate the changes with the effects of in vivo dexamethasone treatment, and to analyze the molecular basis of the changes in gene expression.

METHODS

Culture of rat and human mesangial cells

Rat mesangial cells (RMC) from Sprague-Dawley rats were obtained by enzymatic digestion as described previously [11], and cultured in RPMI 1640 supplemented with 10% fetal calf serum (FCS). Human mesangial cells (HMC) were obtained from Clonetics (San Diego, CA, USA), and cultured in CCMD 180 medium supplemented with 5% FCS.

Proteoglycan synthesis assays

Synthesis of cell-associated and medium-secreted proteoglycans was determined as described by us previously [12]. In brief, quiescent RMC in 24-well plates were transferred into serum-free media for 24 hours. Following serum deprivation, cultures were incubated in RPMI containing ^{3}H-glucosamine (2 μCi/mL) or sulfate-free medium containing ^{35}S-sulfate (5 μCi/mL) in the presence of dexamethasone (1 μmol/L unless otherwise stated) for 48 hours. The medium was harvested and 300 μL of the supernatant was incubated with 25 μL of 25 mmol/L $MgSO_4$, and 120 μL of 2.5% cetylpyridinium chloride (CPC) in the presence of 5 μg of carrier chondroitin sulfate for one hour at 37°C. Precipitated proteoglycans were collected on nitrocellulose filters by vacuum filtration, washed with 1.0% CPC in 20 mmol/L NaCl and radio-counted in a liquid scintillation counter. In some experiments, samples were treated overnight at 37°C with chondroitinase ABC (10 mU) in 33 mmol/L Tris-HCl, 33 mmol/L sodium acetate, 80 μg/mL bovine serum albumin (BSA; pH 8.0), or chondroitinase AC (10 mU) in 33 mmol/L Tris-HCl, 80 μg/mL BSA (pH 6.0), or heparitinase III (10 mU) in 100 mmol/L sodium acetate, 10 mmol/L calcium acetate (pH 7.0) prior to CPC precipitation. For determination of cell-associated proteoglycan synthesis, the cell layers were rinsed with phosphate-buffered saline (PBS) and lysed in 1 mol/L NaOH. Three hundred microliters of each sample were neutralized with 2 N acetic acid, and digested with Pronase E (1 mg/mL) at 55°C for 18 hours. After the addition of chondroitin sulfate (100 μg/mL) as a carrier, cell-associated proteoglycans were precipitated for three hours at 37°C with 1% CPC in 20 mmol/L NaCl. The precipitate was collected on nitrocellulose filters and treated as described above.

Ion-exchange and molecular sieve chromatography

To separate proteoglycans in the media on the basis of differences in charge density, ion-exchange chromatography was performed as described previously using DEAE-Sephacel (Amersham-Pharmacia, Tokyo, Japan) [12]. After application of media containing ^{35}S-sulfate-labeled proteoglycans from control and dexamethasone-treated cells, unbound radioactivity was removed from the column by washing with 30 mL of wash buffer [8 mol/L urea, 50 mmol/L Tris (pH 7.5), 2 mmol/L ethylenediaminetetraacetic acid (EDTA), 0.1 mol/L NaCl, 0.5% Triton X-100]. Bound radioactivity was eluted with a NaCl gradient (0.1 to 0.7 mmol/L in the same buffer) and the radioactivity in the collected fractions was quantified by scintillation counting. To separate proteoglycans on the basis of their hydrodynamic size, the concentrated proteoglycans in peak II were collected and subjected to molecular sieve chromatography using Sepharose CL-2B (Amersham-Pharmacia) following the method of Lee et al [13]. Samples were applied to a 10 mm × 100 cm Sepharose CL-2B column in 4 mol/L guanidine buffer [4 mol/L guanidine, 10 mmol/L EDTA, 0.5% Triton X-100, 50 mmol/L sodium acetate (pH 7.4)] and collected in 0.5 mL fractions. Radioactivity in the eluted fractions was quantified by scintillation counting. The void volume and total volume were assessed using dextran blue and phenol red, respectively [14].

Northern blot analysis

Total RNA was purified from RMC by the acid guanidine-phenol-chloroform method, and quantified by measurement of absorbance of 260 nm in a spectrophotome-

ter. Twenty micrograms of total RNA were denatured with formamide and formaldehyde at 65°C for 10 minutes and fractionated by electrophoresis through a 1.0% formaldehyde-agarose gel. RNA was stained with ethidium bromide to verify integrity and equal loading, transferred to a nylon filter (Pall BioSupport, East Hills, NY, USA), then cross linked using an ultraviolet (UV) irradiator (Stratagene, La Jolla, CA, USA). Prehybridization was conducted at 42°C for two hours in a buffer containing 6 × SSC (0.9 mol/L sodium chloride, 0.09 mol/L sodium citrate, pH 7.0), 5 × Denhardt's solution [0.1% (wt/vol) polyvinylpyrrolidone, 0.1% (wt/vol) ficoll type 400, 0.1% (wt/vol) bovine serum albumin (BSA)], 50% formamide, 0.1% sodium dodecyl sulfate (SDS), and sheared, denatured salmon sperm DNA (100 μg/mL). The cDNA probes for decorin [15] and biglycan [16] were generously provided by Dr. Woessner (Miami University, Miami, FL, USA) and Dr. Dreher (Weis Center for Research, Danville, PA, USA) through Dr. Takagi (Department of Anatomy, Nihon University School of Medicine, Tokyo, Japan). Probes for perlecan and versican were obtained by reverse transcription-polymerase chain reaction (RT-PCR) as described previously [12]. The 1.1 kb human glyceraldehyde-3-phosphate dehydrogenase (GAPDH) probe was purchased from Clontech Laboratories (Palo Alto, CA, USA). Probes were radiolabeled with α-^{32}P dCTP by the random primer synthesis method (RadPrime DNA Labeling System; Gibco BRL, Grand Island, NY, USA). After hybridization, the filter was washed in 0.2 × SSC, 0.1% SDS at 42°C. Bands were visualized, and incorporated radioactivity was quantified by scanning with a laser image analyzer (model BAS 2000; Fuji Film, Tokyo, Japan).

RT-PCR

Reverse transcription-polymerase chain reaction was performed as described by us previously [17]. One microgram of total RNA was reverse transcribed in a reaction mixture containing 10 mmol/L Tris-HCl (pH 8.3), 50 mmol/L KCl, 5 mmol/L $MgCl_2$, 1 mmol/L dNTP, 1 U RNase inhibitor, 2.5 μmol/L (50 pmol) random hexamers and 2.5 U Moloney murine leukemia virus (MMLV) reverse transcriptase in a volume of 20 μL. The reverse transcribed product was amplified with proteoglycan core protein sense and antisense primers in a reaction mixture containing 10 mmol/L Tris-HCl (pH 8.3), 50 mmol/L KCl, 2 mmol/L $MgCl_2$, 0.2 mmol/L dNTP, 15 pmol of each primer, 5 μCi ^{32}P-dCTP, and 2.5 U Taq polymerase using a Perkin-Elmer-Cetus thermal cycler for 24 cycles (Perkin-Elmer, Norwalk, CT, USA). The sequences of the primers for decorin, biglycan, versican, perlecan, and GAPDH were as reported previously [17]. Preliminary experiments confirmed that the amplifications were performed in the linear phase of the amplification cycle. In some experiments, reaction products were subcloned into the plasmid pCDNA3.1His/Topo (Invitrogen, Groningen, The Netherlands) and sequenced using an automated sequencer.

Reaction products were resolved by electrophoresis through 8% polyacrylamide gels. Gels were dried using a gel dryer prior to imaging using a laser image analyzer (model BAS 2000; Fuji Film).

Western blot analysis

Western blot analysis of proteoglycan core proteins was performed following the method of Kaji et al [14] using anti-human decorin (LF-136) and anti-human biglycan (LF-51) antibodies [18, 19], which were generously provided by Dr. Fisher (National Institute of Dental and Craniofacial Research, Bethesda, MD, USA). Proteoglycans in the media of HMC treated with or without dexamethasone were concentrated on 0.3 mL DEAE-Sephacel columns, and then precipitated with 1.3% potassium acetate in 95% ethanol. After digestion with chondroitinase ABC, the samples were subjected to SDS-polyacrylamide gel electrophoresis (SDS-PAGE) on acrylamide 4 to 12% gradient gels, transferred to nitrocellulose membranes and detected using the enhanced chemiluminescence (ECL) Western blotting system (Amersham).

Transient transfection and luciferase assays

Plasmids containing various lengths of the 5′-flanking region of the human biglycan gene cloned upstream of the luciferase gene in vector pGL2-Basic (Promega, Madison, WI, USA) [20] were generously provided by Dr. Ungefroren (University of Hamburg, Hamburg, Germany). The constructs used were Bgn (−1212, +42), Bgn (−985, +42), Bgn (−686, +42), Bgn (−153, +42), Bgn (−46, +42). The numbers in parentheses refer to the positions of the 5′- and 3′-nucleotides relative to the major transcription start site (5′ end of exon 1) of the biglycan gene. To assess the promoter activity of luciferase constructs with and without dexamethasone treatment, RMC in 24-well plates were transfected with various biglycan promoter-luciferase plasmids (0.5 μg) using lipofectamine plus (Gibco-BRL) as recommended by the manufacturer. Some of the cells were treated with dexamethasone (1 μmol/L) after completion of the transfection procedure. A Renilla luciferase construct (pRL-TK) was used to normalize for changes in transfection efficiency, and the luciferase activities were assessed 24 hours after transfection by the dual luciferase assay (Promega) exactly as recommended by the manufacturer.

Protein assays

Protein assays were performed by the Lowry method using a commercially available kit (DC protein assay; Bio-Rad, Hercules, CA, USA).

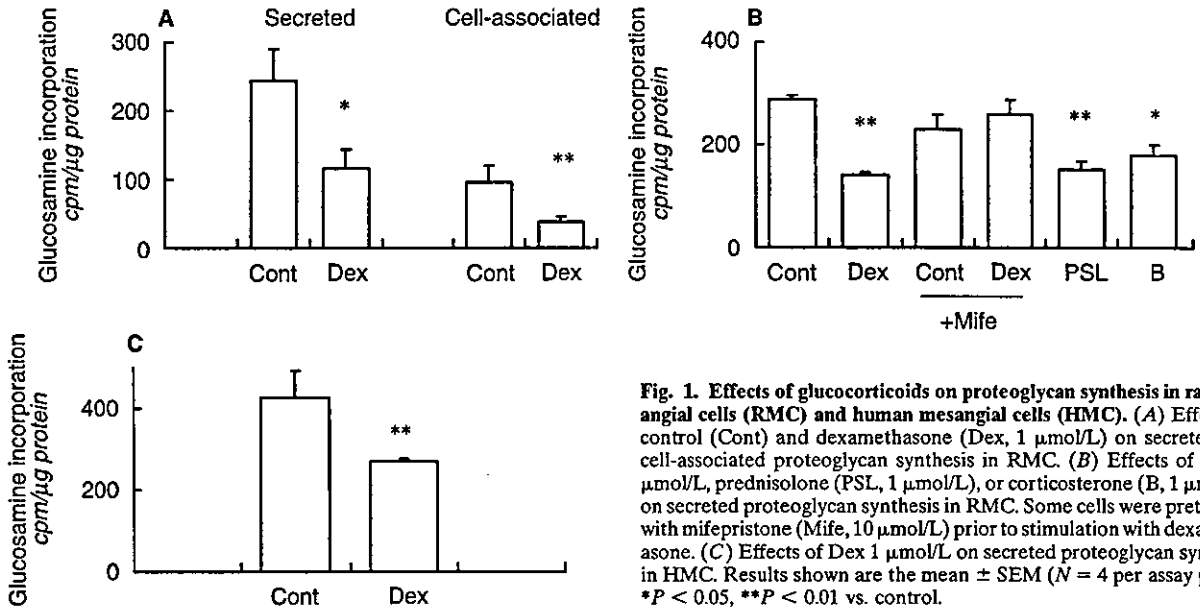

Fig. 1. Effects of glucocorticoids on proteoglycan synthesis in rat mesangial cells (RMC) and human mesangial cells (HMC). (*A*) Effects of control (Cont) and dexamethasone (Dex, 1 μmol/L) on secreted and cell-associated proteoglycan synthesis in RMC. (*B*) Effects of Dex 1 μmol/L, prednisolone (PSL, 1 μmol/L), or corticosterone (B, 1 μmol/L) on secreted proteoglycan synthesis in RMC. Some cells were pretreated with mifepristone (Mife, 10 μmol/L) prior to stimulation with dexamethasone. (*C*) Effects of Dex 1 μmol/L on secreted proteoglycan synthesis in HMC. Results shown are the mean ± SEM ($N = 4$ per assay point). $^*P < 0.05$, $^{**}P < 0.01$ vs. control.

In vivo studies

Ten-week-old male SD rats were treated with or without daily intraperitoneal injections of dexamethasone (5 mg/kg/day) for three days using a previously reported protocol [21]. After euthanasia, the kidneys were removed and glomeruli (>90% purity) were isolated by differential sieving [11]. Total RNA was obtained by the acid guanidine-phenol-chloroform method and subjected to RT-PCR as described above.

Statistics

Results are expressed as the mean ± SEM. Statistical comparisons were made by analysis of variance (ANOVA) followed by Scheffe's F-test. P values less than 0.05 were considered statistically significant.

Materials

Cell culture materials, radioisotopes, and electrophoresis materials were obtained from Gibco-BRL, Amersham International plc, and Bio-Rad, respectively. Other reagents were obtained from Sigma Chemical Co. (St. Louis, MO, USA), unless otherwise stated.

RESULTS

Effects of glucocorticoids on proteoglycan synthesis in RMC and HMC

To examine the effects of glucocorticoids on proteoglycan synthesis, mesangial cells were treated with the glucocorticoid dexamethasone. As shown in Figure 1A, treatment of RMC with dexamethasone resulted in a significant ($P < 0.05$) decrease in both secreted and cell-associated proteoglycan synthesis. To confirm that this action was mediated by the glucocorticoid receptor, experiments were performed with the glucocorticoid antagonist mifepristone (RU-486), as well as the naturally occurring corticosterone and the therapeutic steroid prednisolone. As shown in Figure 1B, the effects of dexamethasone were attenuated by pre-treatment of cells with mifepristone, and mimicked by treatment with corticosterone or prednisolone, suggesting that the changes observed were due to stimulation of the glucocorticoid receptor. Treatment of HMC with dexamethasone caused a similar reduction in proteoglycan synthesis (Fig. 1C).

To assess the dose-dependency and time course of the dexamethasone-induced effects, RMC were treated with various doses of dexamethasone for 24 hours, or with 1 μmol/L dexamethasone for various times. Treatment with dexamethasone caused a dose- and time-dependent reduction of proteoglycan synthesis to approximately 50% of control values after treatment with 1 μmol/L for 24 hours (Fig. 2). In order to characterize the subclass of the proteoglycans in control and dexamethasone-treated samples, conditioned media were treated with the enzymes chondroitinase ABC, chondroitinase AC, and heparitinase prior to CPC precipitation. In the case of ^{35}S-sulfate labeled proteoglycans, treatment with chondrotinase ABC and heparitinase resulted in >95% digestion of the incorporated radioactivity in both control and dexamethasone-treated cells. In the case of ^{3}H-glucosamine, approximately 30 to 35% of the radioactivity remained undigested after treatment with these enzymes (the percentage of the total radioactivity digested by chondroitiniase ABC, AC, hepari-